Analysis of nanofluid due to trapping along a porous annulus with cilia in the presence of thermal radiation

Thesis Submitted By:

SALMA BATOOL (01-248172-013)

Supervised By:

Dr. Rizwan ul Haq

A dissertation submitted to the Department of Computer Science, Bahria University, Islamabad as a partial fulfillment of the requirements for the award of the degree of MS

Session (2017 - 2019)

Bahria University
Discovering Knowledge

MS-13

Thesis Completion Certificate

Scholar's Name: **Salma Batool** Registration N0: **53677**

Programmed of Study: **MS (Mathematics)**

Thesis Title: **Analysis of nanofluid flow due to trapping along a porous annulus with cilia in the presence of thermal radiation**

It is to certify that the above student's thesis has been completed to my satisfaction and, to my belief, its standard is appropriate for submission for Evaluation. I have also conducted plagiarism test of this thesis using HEC prescribed software and found similarity index at **18%** that is within the permissible limit set by the HEC for the MS/MPhil degree thesis.

I have also found the thesis in a format recognized by the BU for the MS/MPhil thesis.

Principal Supervisor's Signature: _____

Date: 15/07/2019 **Name: Dr. Rizwan ul Haq**

Bahria University
Discovering Knowledge

MS-14A

Author's Declaration

I, **Salma Batool** hereby state that my MS thesis titled **"Analysis of nanofluid flow due to trapping along a porous annulus with cilia in the presence of thermal radiation"** is my own work and has not been submitted previously by me for taking any degree from this university **Bahria University Islamabad**, or anywhere else in the country / world. At any time f my statement is found to be incorrect even after my Graduate the University has the right to withdraw/cancel my MS degree.

Name of scholar : **Salma Batool**

Date : 21/06/2019

Bahria University
Discovering Knowledge

MS-14B

Plagiarism Undertaking

I, Salma Batool solemnly declare that research work presented in the thesis titled "Analysis of nanofluid flow due to trapping along a porous annulus with cilia in the presence of thermal radiation" is solely my research work with no significant contribution from any other person. Small contribution / help wherever taken has been duly acknowledged and that complete thesis has been written by me.

I understand the zero tolerance policy of the HEC and Bahria University towards plagiarism. Therefore I as an Author of the above titled thesis declare that no portion of my thesis has been plagiarized and any material used as reference is properly referred / cited.

I undertake that if I am found guilty of any formal plagiarism in the above titled thesis even after award of MS degree, the university reserves the right to withdraw / revoke my MS degree and that HEC and the University has the right to publish my name on the HEC / University website on which names of students are placed who submitted plagiarized thesis.

Student / Author's Sign: _____

Name of the Student: **Salma Batool**

Dedicated to

Muhammad (sallallahu alaihi wasallam)

Who is forever a constant source of guidance, a source of knowledge and blessing for entire creation

My worthy parents and respected teachers

whose prays and support have always been a source of inspiration and encouragement for me

Acknowledgments

I am thankful to Almighty **ALLAH** the most beneficent and the most merciful, who granted me the ability and potential to fulfill the requirements of my thesis. I offer my humble gratitude and love to the Holy Prophet Muhammad (peace be upon him), Ahhl e bait and Sahaba e karaam whose lives and teachings are the source of knowledge and guidance for humanity.

First of all, I would like to express my sincere appreciation for my supervisor, **Dr. Rizwan ul Haq** for serving as my advisor and shearing his knowledge of mathematics with me. He was available to me all the time and provided me a nice work atmosphere in the office. He has encouraged a lot throughout my research work and tried his level best to answer my quires. I could not have imagined having better advisor and mentor for my study.

Besides my supervisor I would like to thank **Dr. Muhammad Ramzan** and **Dr. Jafar Hasnain**who have always been supportive in all of my course work and kept encouraging me throughout the session in Bahria University, Islamabad Campus.

I am very thankful to my parents for their support and guidance.Their love, encouragement and desire to see me succeed at every turn of this winding path were immeasurable. I am wholeheartedly grateful to all my sincere friends and class fellows specially Ali, Adeela Mubeen and Syed Saqib Shah, Hammad Shah and Umar Ali Shah for supporting me, offering valuable advice and especially for guidance during the process of writing thesis.

Salma Batool

Bahria University Islamabad, Pakistan

Abstract

The main aim of the thesis is to analysis the nanofluid flow due to trapping along porous annulus with cilia in the presence of thermal radiation effects. The structure of the thesis consist of five chapters that includes review work and the extension. In the first Chapter introduction and literature work is discussed. In chapter two, basic definitions and fundamental laws which are used for mathematical modelling are defined. Chapter three contains the review work done by S. Nadeem and H. Sadaf [17]. For representation of solution graphs are also drawn in this chapter. Chapter four is extension of review work, by adding porous media for annulus and thermal radiation effects. Cylindrical coordinates have selected for mathematical formulation of the flow problem. This formulation consist of continuity equation, momentum equation and energy equation. Exact solutions are obtained and compared with numerical solution. A detailed analysis of model is presented through graphs. These graphs are constructed for different physical parameters. Chapter five contains the conclusion of review and extension work.

Contents

List of Figures

List of Tables

Chapter 1

Introduction and literature review

The word Peristaltic originates from Greek word "Peristaltikos" , which implies fastening and packing. Peristalsis is an instrument to direct liquids by methods for moving constrictions on the tube divider. Peristalsis is the result of many coordinated contractions of the longitudinal and transverse muscles in the walls of a tubular organ. Peristaltic flow refers to the transport of fluid in a channel by the act of flexible walls. A single peristaltic wave takes the form of circular constriction around the lumen that moves along the length of the organ. The walls of the organ are always slightly relaxed before the arrival of the constriction, so that the wave appears to push the contents in the direction in which it travels. Peristaltic wave follows each other continuously at a fixed rhythm and rate. In man, for example, the peristaltic rhythm of the stomach is 3 waves/min. Intestinal peristalsis occurs at the rate of 6 waves/min. Peristalsis is engaged with gulping nourishment through the throat, transport of chyme in small digestive tract, transport of bile. There are numerous other critical uses of peristalsis, for example, the outline of roller pumps which are helpful in drawing liquids without tainting because of contact with the pumping apparatus. Many biomedical devices such as dialysis machine, open heart bypass pump machine are designed on the mechanism of peristalsis.

Latham [1] was first who made study for peristaltic flow. Later on Shapiro [2] explained this phenomenon in two dimensional flow. He considered the flow as inertia free with small wave length. Barton and Raynor [3] discuss peristaltic motion of two dimensional flow in tubes. They take assumption of small Reynolds number. Shapiro et al. [4] talked about the

peristaltic flow for both planar and axisymmetric cases. They apply the condition of long wave length and very small Reynolds number. Yin and Fung [5] studied peristaltic pumping in coordinate channel and axisymmetric tube. They assume the condition of small wave length and low Reynolds number. Jaffrin [6] examined the inertia and streamline curvature impact on peristaltic flow. Jaffrin and Shapiro [7] represented peristaltic flow in distinctive routines. They studied peristaltic motion in existence of pressure gradient. For circular cylindrical tubes peristaltic pumping is deliberated by Takabatake et al [8]. In other study Mekhiemer [9] examined the peristaltic flow of couple stress in an annulus with an endoscope.

The term cilia are regularly utilized for 'Eukaryotic Cell'. It is gotten from the "eyelashes". Cilia is infinitesimal, cylinder and thread like structure. Single cilium can be measured on (1-10) micrometer long and less than 1 micrometer wide. The state of the cilia components is particularly like hair. Cilia movement assume a crucial job in different physiological procedures, for example, propagation nourishment locomotion respiration and growth. There are two types of cilia, motile and non-motile. Motile cilia are present on surface of tissues and are responsible for protecting a person from germs. Non-motile cilia are responsible for sensing the surrounding environment. Cilia transport physiological liquids along the epithelium, the covering of the hole of structures all through the body. Cilia are basically present in the sensory system, stomach related framework, male and female regenerative framework.

Agrawal and Anawar-ud-din [10] talked about cilia transference of biofluid with variable thickness. Barton and Raynor [11] discussed mucou flow due to motion of cilia. [12, 13] analysed hydrodynamics of protozoa that they utilize cilia for movement . Velez – cordero and Lauga [14] explained the

envelop model of cilia by taking newtonian fluid . Mechanical features of cilia are presented by Rydholm et al [15]. Basten and Giles [16] discussed function of cilia.

Recently [17] examined flow rate analysis of nanofluid enclosed in annulus with cilia motion. Keeping above mentioned efforts, research work done by S. Nadeem and Hina Sadaf will extended by porous annulus and presence of thermal radiation. This work has not yet been explored in literature.

Nomenclature

Velocity components are U, V.

Volume fraction of the nano particle is represented by ϕ.

Temperature of outer tube is represented by T_1.

Heat capacity of solid particle is denoted as $(\rho c_p)_p$.

a_1 is radius of inner tube.

Nanofluid density is represented by ρ_{nf}.

μ_{nf} shows the viscosity of nano fluid.

$(\rho c_p)_f$ shows the heat capacity of fluid.

Viscosity of fluid is represented by μ_f.

c is wave speed.

λ represent the wave length

Heat capacity of solid particle is represented by $(\rho c_p)_p$

Z_0 shows the reference position of the tip.

Measure of eccentricity is represented by α.

Inner tube temperature is T_0.

a_2 is radius of outer tube.

Conductivity of nanofluid is denoted by k_{nf}.

B represent the heat source or sink parameter.

Conductivity of the fluid is denoted by k_f.

k_s is conductivity of particle.

Heat absorption constant is represented by Q_0.

Chapter 2

Elementary concepts of fluid

In this section some essential definitions well defined laws have been discussed.

2.1 Mechanics

It is the most established physical science that deals with both stationery and moving limits affected by powers. The part of the mechanics that deals with bodies very still is considered statics while dynamics is the branch that deal with bodies in movement.

2.2 Fluid

It is a substance with the property of altering shape with application of stress.

2.3 Fluid mechanics

It is is branch of physics that deals with various characteristics of fluid both in rest and in motion are discussed.

2.4 Physical properties of fluid

Here are some properties of fluid are discussed.

2.4.1 Density

It is the proportion between mass(m) and volume (v) of a fluid. Mathematically,

$$\rho = \frac{mass}{volume}$$

2.4.2 Pressure

It is rate of change of force per unit area. Mathematically,

$$P = \frac{force}{area}$$

2.4.3 Viscosity

The shear stress on a fluid with some rate of deformation is called dynamic viscosity

$$\mu = \frac{shear\ stress}{deformation\ rate}$$

2.4.4 Temperature

Temperature is motion of molecule from high temperature to lower temperature due to inertial forces.

2.5 Types of fluid

2.5.1 Ideal fluid

It is fluid having zero resistance at every point.

2.5.2 Real fluid

It is fluid having non zero resistance at every point.

2.5.3 Newtonian fluid

The fluid which follow Newton's law of viscosity is called newtonian fluid. Examples of Newtonian fluid are air and water etc. Mathematically,

$$\tau_{yx} = \mu \frac{du}{dy}$$

2.5.4 Non-Newtonian fluid

If shear stress is not linearly proportional to deformation rate, then fluid is non-newtonian

$$\tau_{yx} = k\left(\frac{du}{dy}\right)^n$$

for $n \neq 1$,

2.5.5 Incompressible fluid

The fluid in which the volume and thus density of flowing fluid does not changes during flow. Mathematically it can be expressed as

$$\rho \neq \rho(x, y, z, t)$$

.

2.5.6 Compressible fluid

The fluid in which the volume and thus the density of the flowing fluid changes during flow. Mathematically it can be express as

$$\rho = \rho(x, y, z, t)$$

.

2.5.7 Steady fluid

When there is no change in fluid property at point with time, then it implies as steady fluid. Mathematically

$$\frac{\partial \eta}{\partial t} = 0$$

.

2.5.8 Unsteady fluid

When there is change in fluid property at point with time, then it implies as steady fluid. Mathematically

$$\frac{\partial \eta}{\partial t} \neq 0$$

.

2.6 Nanofluid

Nanofluids are another gathering of nano technologies based liquids made by dispersing nanometer estimated molecule with typical length scale on request of (1-100nm) in standard heat transfer fluids. These particles can be found in the metal such as (Cu, Al), oxides (Al_2O_3) or non-metal (Nano tubes, Carbon, Graphite)

2.7 Magnetohydrodynamics

A branch of study in which the effect of magnetic field is discussed on an electrically conducting fluid.

2.8 Viscous dissipation

It is a physical phenomenon which represents the contribution of viscous forces in heat dissipation or heat transfer.

2.9 Mixed convection

The phenomenon in which natural as well as forced convection mechanisms contribute together to transfer heat is known as mixed convection.

2.10 Stream function

A type of function in which farm of flow pattern is discussed is called stream function. It is the discharge per unit thickness. In case of incompressible fluid stream function is used to explain the flow field in terms of volume flow. In

case of incompressible it is used to express flow field in term of mass flow rate.

2.11 Porous medium

A solid substance contains valid space or pores which are distributed randomly. Examples are humans skin, wood, sand and cloth etc.

2.12 Types of forces

2.12.1 Body forces

A force acting all through the volume of a body with no physical contact. Gravity and electromagnetic forces are examples.

2.12.2 Surface forces

Force that acts across an internal and external element in a body through direct physical contact. Pressure and shear forces are examples of surface forces.

2.12.3 Inertia forces

A force which resists a change in state of an object.

2.13 Non dimensional parameters

Some of the non-dimensional parameters of physical interest encountered in this work are explained.

2.13.1 Reynold number

Ratio of inertia forces to viscous force is defined to be as Reynold number. Physically it determine the behaviour, weather flow is laminar or turbulent. For turbulent flow Re is large while it is smaller for laminar flow. Mathematical farm is

$$Re = \frac{Vh\rho}{\mu}$$

. where ρ is fluid density, V is the velocity, h stand for distance and μ is dynamic viscosity.

2.13.2 Eckert number

It is ratio of advective transfer and heat dissipation potential. It is mathematically expressed as

$$Ec = \frac{V^2}{\Delta T c_p}$$

2.13.3 Grashof number

This number is significant in characterizing mixed convection effects and it is defined as ratio of buoyancy to viscous forces acting upon the fluid. It can be expressed as;

$$G_r = \frac{g\beta_T(T_1 - T_0)L^3}{\nu^2}$$

.

2.13.4 Wave number

It is ratio between width(a) of the channel and wave length(δ). In farm of mathematics

$$\lambda = \frac{a}{\delta}$$

.

Chapter 3

Flow rate analysis of nanofluid enclosed in an annulus with cilia

3.1 Introduction

In this chapter, review work is established that is already published by S.Nadeem and Hina sadaf [17], on the study of nanofluid flow through a concentric annulus. Cilia effects are also considered to determine the flow analysis adjacent to the annulus walls. Mathematical model considered as movement of cilia in presence of endoscopic tube. Outer tube is taken as metachronal wave and inner tube taken as rigid. Initially, we formulated governing equations of the flow. Mathematical formulation of problem is taken in cylindrical coordinate. First we convert system of leading PDEs into dimensionless ODEs. Exact solution is calculated and analysed by graphs and their discussion.

3.2 Formulation of model

Consider movement of cilia for 2-D flow of an incompressible viscous nanofluid in an annulus.

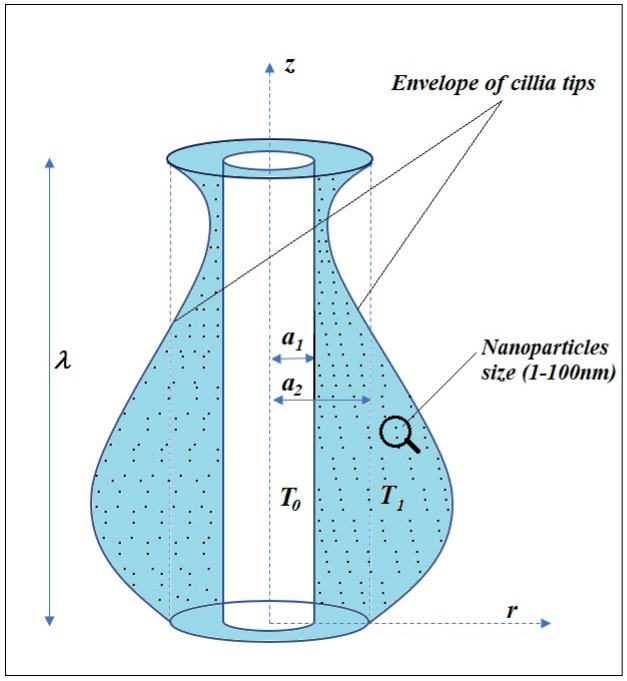

Fig. 1: Geometry of model

Continuity and momentum equations can be formulated:

$$\hat{U}_{\hat{R}} + \frac{\hat{U}}{\hat{R}} + \hat{W}_{\hat{Z}} \quad = 0 \tag{3.1}$$

$$\rho_{nf}\ \left(\hat{U}_{\hat{t}} + \hat{U}\hat{U}_{\hat{R}} + \hat{W}\hat{U}_{\hat{Z}}\right) = -\ \hat{P}_{\hat{R}} + \ \mu_{nf}\ \left(\frac{1}{\hat{R}}\hat{U}_{\hat{R}} + \hat{U}_{\hat{R}\hat{R}} - \ \frac{\hat{U}}{\hat{R}^2} + \hat{U}_{\hat{Z}\hat{Z}}\right) \tag{3.2}$$

$$\rho_{nf}\ \left(\hat{W}_{\hat{t}} + \hat{U}\hat{W}_{\hat{R}} + \ \hat{W}\hat{W}_{\hat{Z}}\right) = \ -\hat{P}_{\hat{Z}} + \ \mu_{nf}\ \left(\frac{1}{\hat{R}}\hat{W}_{\hat{R}} + \hat{W}_{\hat{R}\hat{R}} + \hat{W}_{\hat{Z}\hat{Z}}\right) + \left(\rho\beta\right)_{nf}\ \hat{g}\ \left(\hat{T} - T_1\right) \tag{3.3}$$

$$(\rho\, c_p)_{nf}\ (\hat{T}_{\hat{t}} + \ \hat{U}\hat{T}_{\hat{R}} + \ \hat{W}\hat{T}_{\hat{Z}}) = k_{nf}\ (\frac{1}{\hat{R}}\hat{T}_{\hat{R}} + \hat{T}_{\hat{R}\hat{R}} + \hat{T}_{\hat{Z}\hat{Z}}) + Q_0 \tag{3.4}$$

Heat capacity and thermal conductivity of nanofluid express as fol-

low [18, 19]

$$\alpha_{nf}(\rho c_p)_{nf} = k_{nf}, \quad \mu_{nf}(1-\phi)^{2.5} = \mu_f, \quad \frac{\rho_{nf}}{\rho_f} = \phi\,(\frac{\rho_s}{\rho_f} - 1) + 1$$

$$\frac{(\rho\beta)_{nf}}{\rho_f\beta_f} = (1-\phi)+\phi\frac{\rho_s\beta_s}{\rho_f\beta_f}, \quad \frac{(\rho c_p)_{nf}}{(\rho c_p)_f} = 1+\phi\,(\frac{(\rho c_p)_s}{(\rho c_p)_f} - 1) \tag{3.5}$$

$$k_{nf}((k_s + 2k_f) + \phi(k_f - k_s)) = k_f((k_s + 2k_f) - 2\phi(k_f - k_s))$$

Table 1: Thermo physical characteristics of nanoparticles and fluid

Physical characteristics	Copper	Pure blood
$c_p(\frac{J}{kgK})$	385	3594
$\rho(\frac{kg}{m^3})$	8933	1063
$k(\frac{W}{mk})$	400	0.492
$\beta.10^{-5}(\frac{1}{K})$	1.67	0.18

Mathematically envelope of ciliated tips can be express:

$$\hat{R} = \hat{g}(\hat{Z}, \hat{t}) = [a_2 + a_2\, \epsilon\, cos(\frac{2\pi}{\lambda} Z^*)] = \hat{R}_2 \tag{3.6}$$

Cilia move in different ways examined by Sleigh [20] so consider their position in vertical ways which can be expressed :

$$\hat{Z} = \hat{h}(\hat{Z}, \hat{Z}_0, \hat{t}) = \hat{Z}_0 + a_2 \alpha \epsilon sin(\frac{2\,\pi}{\lambda} Z^*) \tag{3.7}$$

The perpendicular and parallel velocities of cilia are

$$\hat{W} = \frac{\partial \hat{Z}}{\partial \hat{t}} = \frac{\partial \hat{h}}{\partial \hat{t}} + \frac{\partial \tilde{h}}{\partial \hat{Z}} \frac{\partial \hat{Z}}{\partial \hat{t}} = \frac{\partial \hat{h}}{\partial \hat{t}} + \frac{\partial \hat{h}}{\partial \hat{Z}} \hat{W} \tag{3.8 a}$$

$$\hat{U} = \frac{\partial \hat{R}}{\partial \hat{t}} = \frac{\partial \hat{g}}{\partial \hat{t}} + \frac{\partial \hat{g}}{\partial \hat{Z}} \frac{\partial \hat{Z}}{\partial \hat{t}} = \frac{\partial \hat{g}}{\partial \hat{t}} + \frac{\partial \hat{g}}{\partial \hat{Z}} \hat{W} \tag{3.8 b}$$

Solving Eqs. (3.6−3.8) we get

$$\hat{W} = \hat{\chi}(\hat{Z},\ \hat{t}) = \frac{\frac{-2\pi}{\lambda} a_2 c \epsilon \alpha\ \ cos(\frac{2\pi}{\lambda} Z^*)}{1 - \frac{2\pi}{\lambda} a_2 \epsilon \alpha\ \ cos(\frac{2\pi}{\lambda} Z^*)} \tag{3.9 a}$$

$$\hat{U} = \frac{\frac{2\pi}{\lambda} a_2 c \epsilon\ \ sin(\frac{2\pi}{\lambda} Z^*)}{1 - \frac{2\pi}{\lambda} a_2 \epsilon \alpha\ \ cos(\frac{2\pi}{\lambda} Z^*)} \quad \text{at} \quad \hat{R} = \hat{R}_2 \tag{3.9 b}$$

Following transformations are used

$$\hat{r} = \hat{R} \quad , \quad \hat{z} = Z^* \quad , \quad \hat{u} = \hat{U} \quad , \quad \hat{w} = \hat{W} - c \tag{3.10}$$

where $Z^* = \hat{Z} - c\hat{t}$.

Boundary conditions are defined in this farm

$$\hat{W} = 0 \quad \text{at} \quad \hat{R} = \hat{R}_1$$
$$\hat{W} = \hat{\chi}(\hat{Z}, \hat{t}) \ \text{ at } \ \hat{R} = \hat{R}_2 = \ a_2 + a_2\epsilon \cos(\tfrac{2\pi}{\lambda} Z^*) \tag{3.11}$$

Non dimensional variables are defined as:

$$R = \frac{\hat{R}}{a_2}, \quad p = \frac{a_2^2 \hat{p}}{c\lambda\mu_f}, \quad r = \frac{\hat{r}}{a_2}, \quad \delta = \frac{a_2}{\lambda}, \quad Z = \frac{\hat{Z}}{\lambda}, \quad t = \frac{c\hat{t}}{\lambda}, \quad Re = \frac{ac\rho_f}{\mu_f}$$

$$u = \frac{\lambda\hat{u}}{a_2 c}, \quad W = \frac{\hat{W}}{c}, \quad w = \frac{\hat{w}}{c}, \quad r_1 = \frac{\hat{r}_1}{a_2} = \frac{a_1}{a_2} = \xi, \quad \theta = \frac{\hat{T} - \hat{T}_1}{\hat{T}_0 - \hat{T}_1} \ , \ U = \frac{\lambda\hat{U}}{a_2 c}$$

$$B = \frac{Q_0 a^2}{k_f(\hat{T}_0 - \hat{T}_1)} \quad , \ G_r = \frac{g \ \beta_f \ \rho_f \ a^2(\hat{T}_0 - \hat{T}_1)}{c\mu_f}, \qquad r_2 = \frac{\hat{r}_2}{a_2} = 1 + \epsilon \ cos(2\pi z) \tag{3.12}$$

After using dimensionless parameter, applying the condition of low Reynolds number, long wave length approximation and transformation defined in Eqs. (3.10) and (3.12) Eqs. (3.2−3.4) becomes

$$p_r \ = \ 0 \tag{3.13}$$

$$-p_z + \frac{\mu_{nf}}{\mu_f}(w_{rr} + \frac{1}{r}w_r) + \frac{(\rho\beta)_{nf}}{(\rho\beta)_f} G_r\theta = 0 \tag{3.14}$$

$$\frac{\alpha_{nf}}{\alpha_f}(\frac{1}{r}\theta_r + \theta_{rr}) + B\frac{(\rho c_p)_f}{(\rho c_p)_{nf}} = 0 \tag{3.15}$$

Boundary conditions after dimensionless parameters are

$$w = -1-2\pi\epsilon\alpha\delta cos(2\pi z) \text{ at } r = r_2 \tag{3.16}$$

$$w = -1 \text{ at } r = r_1 \tag{3.17}$$

$$\theta = 1 \text{ at } r = r_1 \ , \theta = 0 \text{ at } \quad r = r_2 \tag{3.18}$$

$$u = 2\pi\epsilon \sin(2\pi z)+(2\pi)^2\epsilon\alpha\delta \cos(2\pi z)sin(2\pi z) \text{ at } r = r_2 \tag{3.19}$$

3.3 Obtained results

Solution of the boundary values problem (3.14−3.19) is directly noted:

$$\theta = -d_3\frac{r^2}{4} + d_4\, Log(r) + d_5 \tag{3.20}$$

$$\begin{aligned} w \ = \ & \frac{1}{16(Log(r_1) - Log((r_2))}(Log(r_1)(16\chi(z)-d_8r^2+d_8{r_2}^4-16d_{11}(-r^2+{r_2}^2)) \\ & +Log(r_2)(16 + d_8r^4 - d_8{r_1}^4 - 16d_{11}(+r^2 - {r_1}^2) - 4d_9(+{r_1}^2 - r_2^2)Log(r_1)) \\ & +(-16 + d_8{r_1}^4 - d_8{r_2}^4 + 16d_{11}(-{r_1}^2 + r_2^2) + 4d_9((-r^2 + {r_1}^2)Log(r_1) \\ & -16\chi(z))Log(r))+ \frac{dp}{dz}\ \frac{-1}{4d_6(Log(r_2) - Log(r_1))}((-{r_1}^2+r_2^2)Log(r)-(r^2-{r_1}^2)Log(r_2) \\ & -(-r^2+{r_2}^2)Log(r_1) \end{aligned} \tag{3.21}$$

where

$$d_1 = \frac{\alpha_f}{\alpha_{nf}}, \qquad d_2 = \frac{(\rho c_p)_f}{(\rho c_p)_{nf}}, \quad d_3 = Bd_1d_2, \quad d_4 = \frac{-d_3{r_2}^2 + 4 + d_3{r_1}^2}{4(Log(r_2) - Log(r_1))}$$

$$d_5 = \frac{-d_3{r_2}^2Log(r_1) + d_3{r_1}^2Log(r_2) + 4Log(r_2)}{4(Log(r_2) - Log(r_1))}, \quad d_6 = \frac{\mu_{nf}}{\mu_f}, \quad d_7 = (1-\phi)+\phi\frac{(\rho\beta)_s}{(\rho\beta)_f}$$

$$d_8 = -\frac{d_3G_rd_7}{4b_6}, \quad d_9 = \frac{d_4G_rd_7}{d_6}, \quad d_{10} = \frac{d_5G_rb_7}{d_6}, \quad d_{11} = \frac{3d_9}{8} - \frac{d_{10}}{4}$$

By using the following relations we get pressure gradient

$$F_g = \int_{r_1}^{r_2} (rw)dr \tag{3.22}$$

Pressure gradient is

$$\frac{dp}{dz} = \frac{F_g - p_1}{p_2} \tag{3.23}$$

Velocities and flow rate in non dimension form in term of stream function relation can be written :

$$Q = F_g + \frac{1}{2}(1 + \frac{\epsilon^2}{2} - \xi^2) \tag{3.24}$$

$$u = -\frac{1}{r}\frac{\partial \Psi}{\partial z} \quad w = \frac{1}{r}\frac{\partial \Psi}{\partial r} \quad at\ r = r_2 \tag{3.25}$$

3.4 Graphical results

3.4.1 Velocity profile

This section illustrates the graphs of solution obtained for velocity. Profile of velocity is plotted against radial axis r in Figs. (2 - 3) for different values of volume fraction of the nanoparticle and Grashof number. Figs. (2 - 3) show by higher values of ϕ and G_r velocity profile also rise in the range of $r \in [0.1, 0.6]$ close to endoscopic tube. Velocity profile decreases close to cilia tips. Fig. (2) explains that when nanoparticle concentration is added into base fluid, velocity profile extended close to endoscopic tube. Fig. (3) determines that buoyancy forces assume a prevailing job close endoscopic tube is due to the velocity profile rises close to the endoscopic tube. Viscous powers assume

a important role close tips of cilia so the velocity profile adds to diminish.

3.4.2 Temperature Profile

Figs. (4 - 5) represent temperature profile for distinct values of B (heat source) and volume fraction of nanoparticle. Fig. (4) indicates that temperature profile rise with rising values of B. On other hand with increasing values of ϕ temperature profile declines. Fig. (5) describes that fluid temperature decreases with increasing nano particle. For quick dissipation high thermal conductivity of nanoparticle assume imperative role. Different type of copper nanoparticle can be used as coolant.

3.4.3 Pressure gradient

Figs. (6 -8) represent graph of dp/dz for distinguish values of ϵ, ϕ, and G_r. It has been observed from Figs. (6 - 8) that pressure gradient obtained higher range in narrow part of annulus in domain $z \in [0.75, 1.26]$ and take small values in wider portion of annulus in domain $z \in [0.26, 0.74]$ and $z \in [1.27, 1.74]$. In wider part of annulus flow can easily pass. But in narrow part of tube more dp/dz is needed to attain same flux.

3.4.4 Pressure rise

Figs. (9 - 10) are plotted to see the behaviour of the solid volume fraction of the nanoparticle, cilia length parameter, and Grashof number on the pressure rise for different values. Fig. (9) explains that Δp extended in range $Q \in$ [-1, 0.4] with extending value of cilia length parameter and decreases in rest of region. Fig. (10) illustrates pressure rise stretch in region $Q \in [-1, 0.05]$ for largest values of ϕ and decline in remaining part of annulus.

3.4.5 Streamlines

The trapping phenomenon for distinguish values of length of cilia and volume fraction of nano particle is discussed by Figs. (11 - 16). Streamlines for volume fraction of nano particles are represented by Figs. (11 - 13). Figs. (14 - 16) represent streamlines for distinguish values of cilia length. By rising values of ϕ, number of trapped bolus reduced. By rising values of cilia length size of bolus decline but number of bolus is fixed. By using theses figures we can judge that ciliated tips help movement of fluid so so the trapped boluses show up close to the right divider when contrasted with the left endoscopic divider because of the more circulation of the liquid.

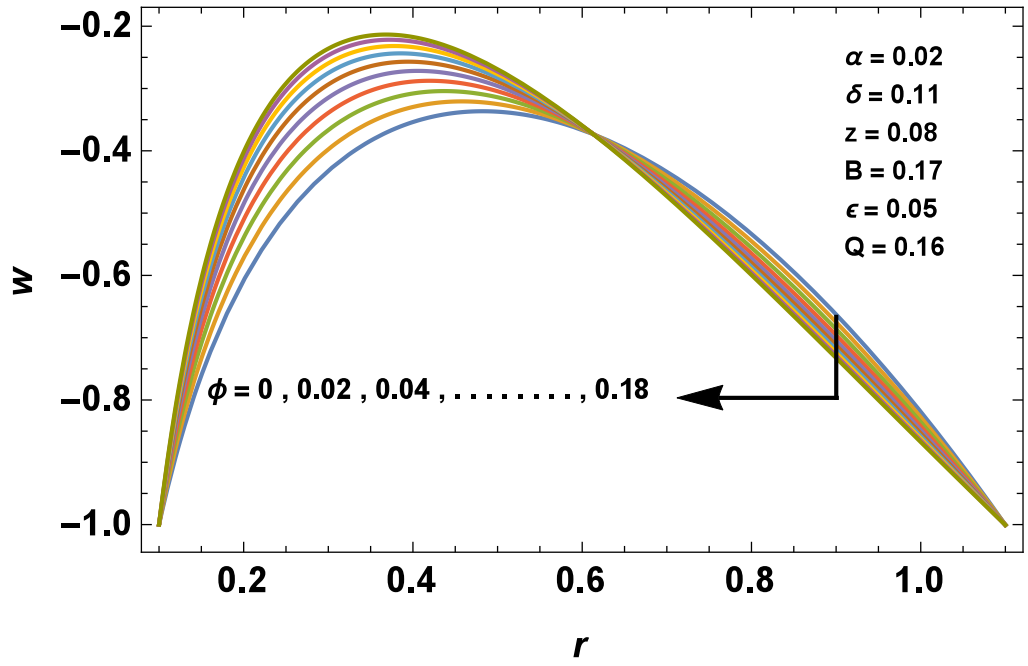

Fig. 2: Velocity profile for variation of ϕ

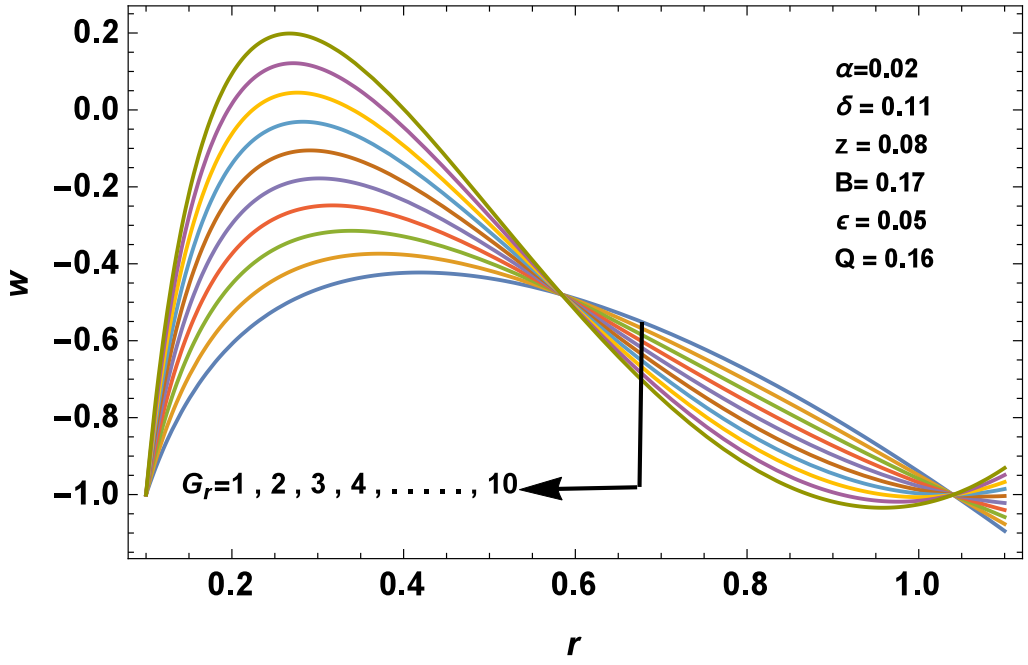

Fig. 3: Velocity profile for variation of G_r

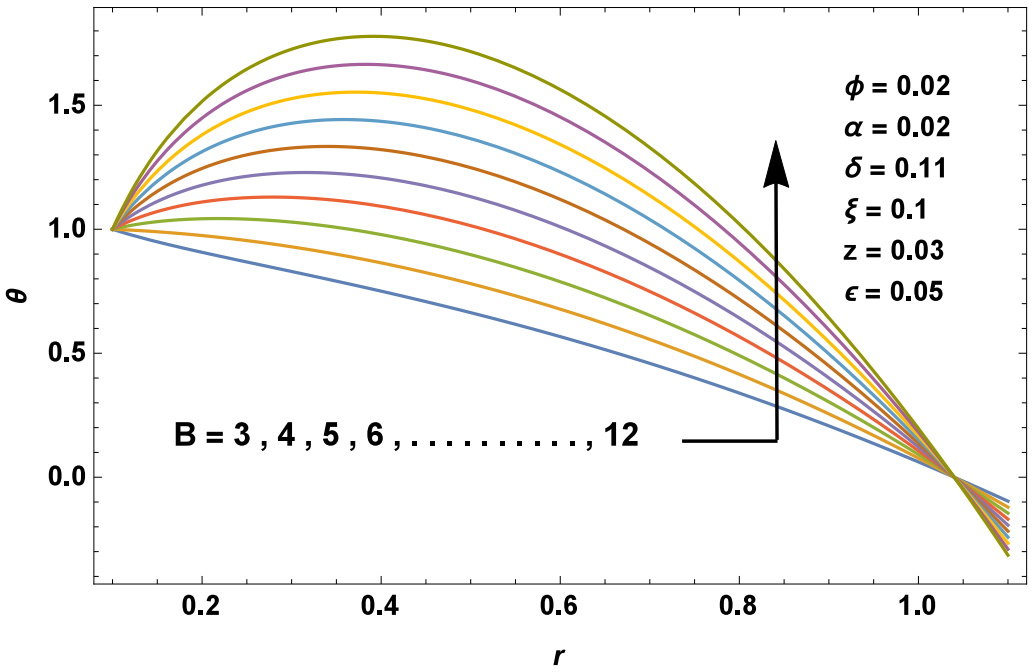

Fig. 4: Profile for temperature w.r.t B

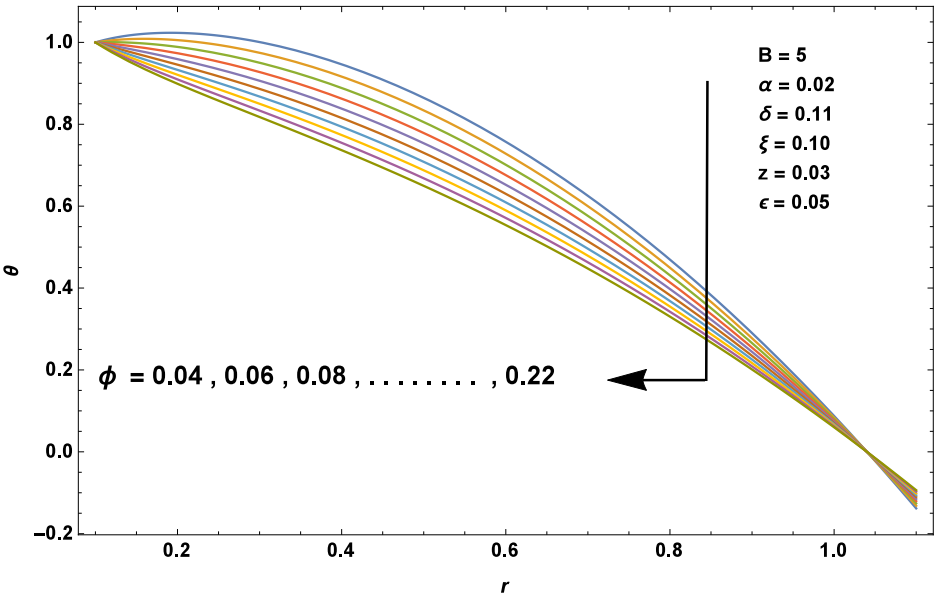

Fig. 5: Profile for temperature w.r.t ϕ

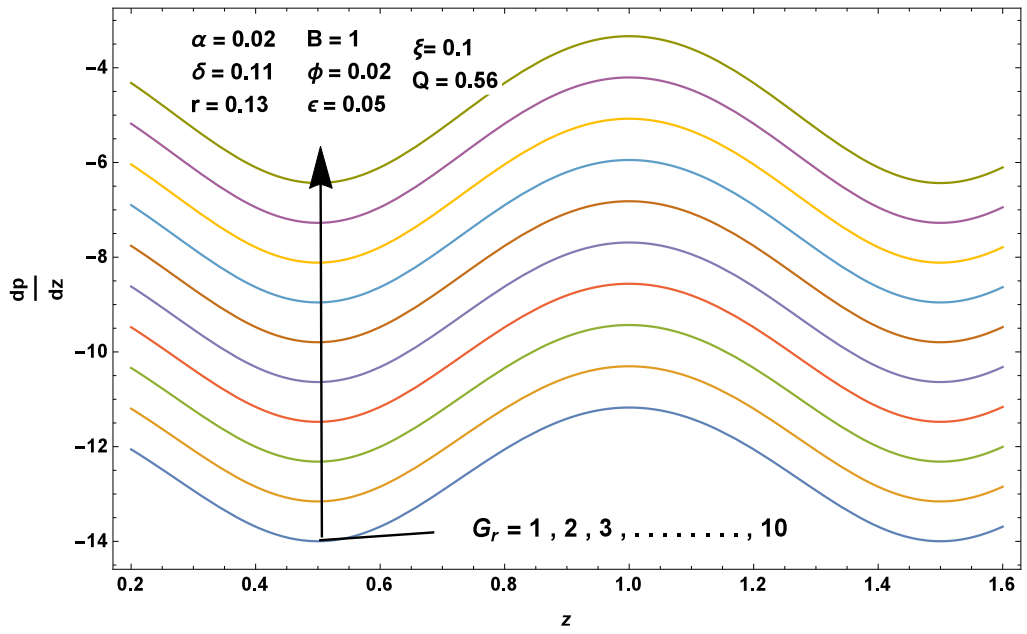

Fig. 6: Pressure gradient for variation of G_r

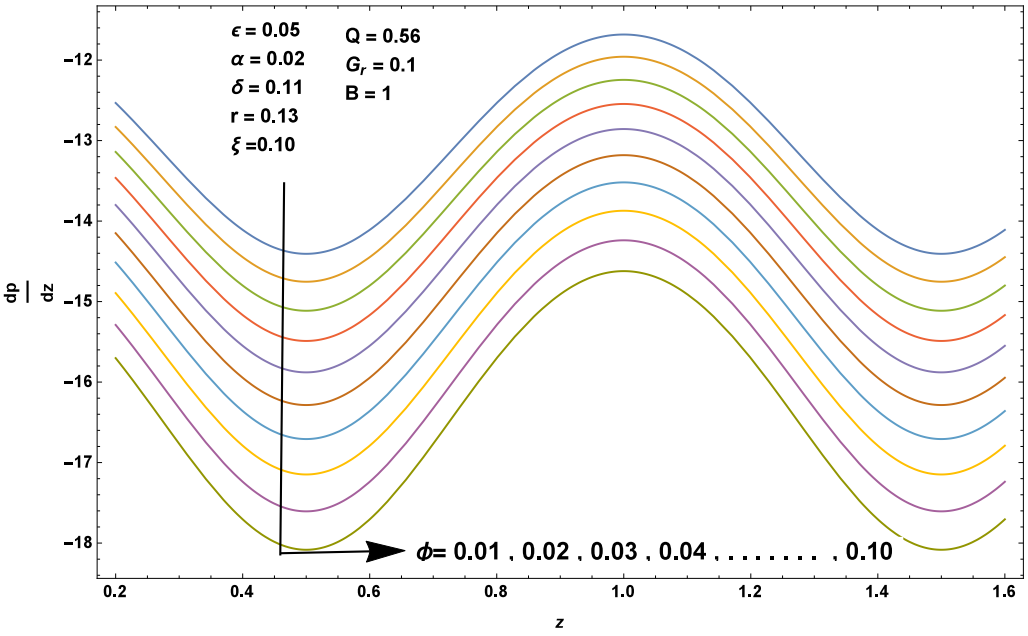

Fig. 7: Pressure gradient for variation of ϕ

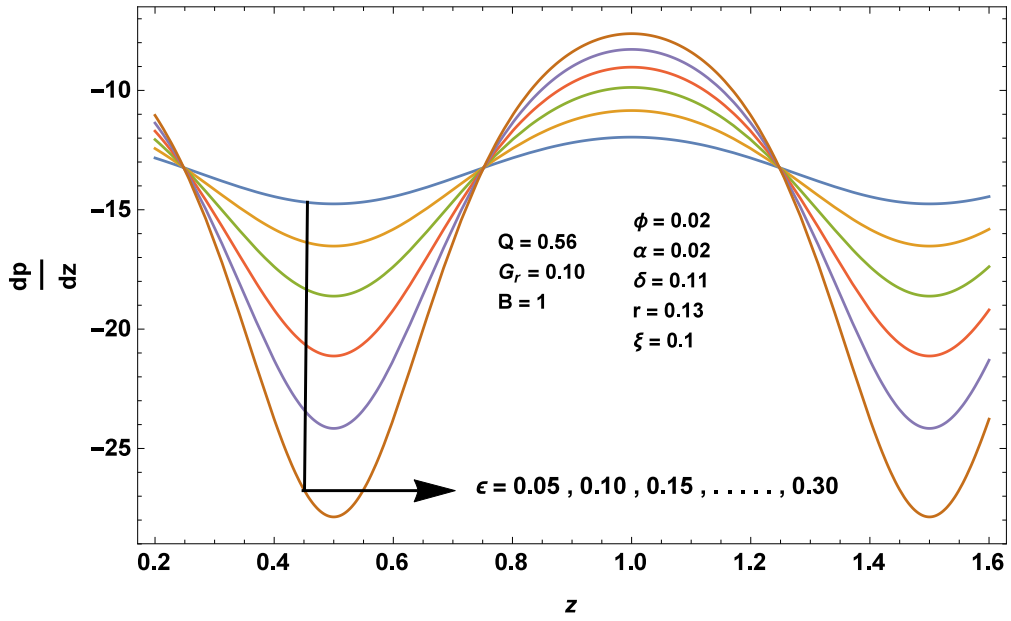

Fig. 8: Pressure gradient for variation of ϵ

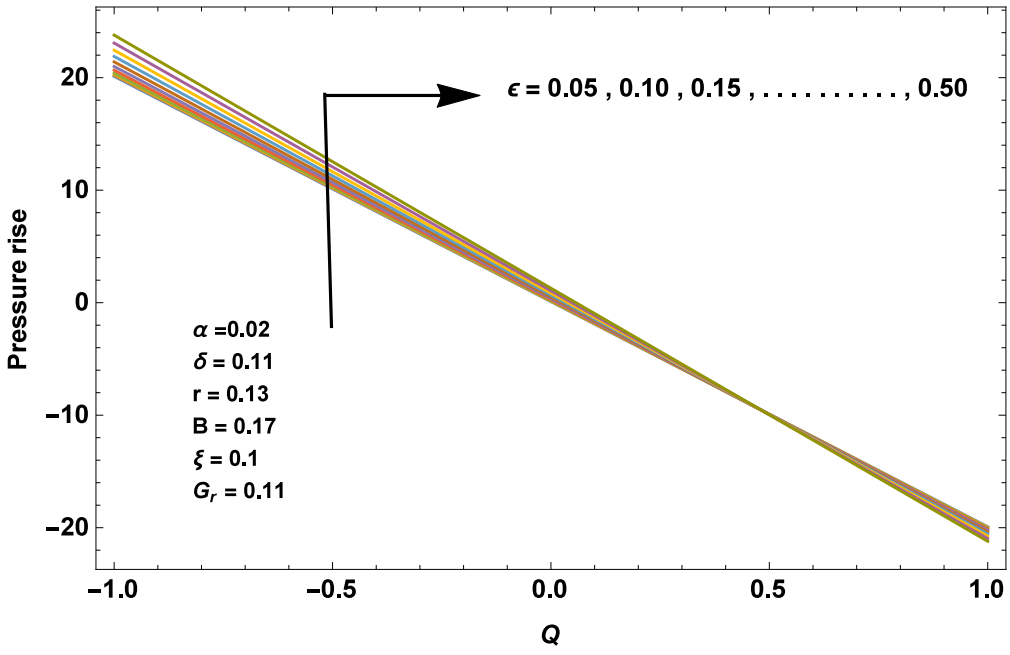

Fig. 9: Pressure rise for variation of ϵ

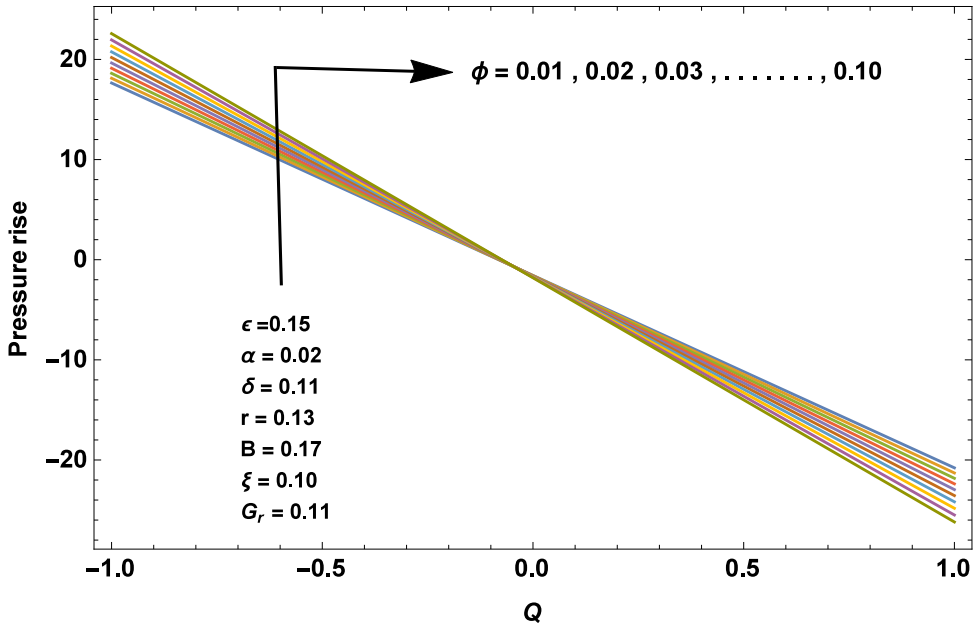

Fig. 10: Pressure rise for variation for ϕ

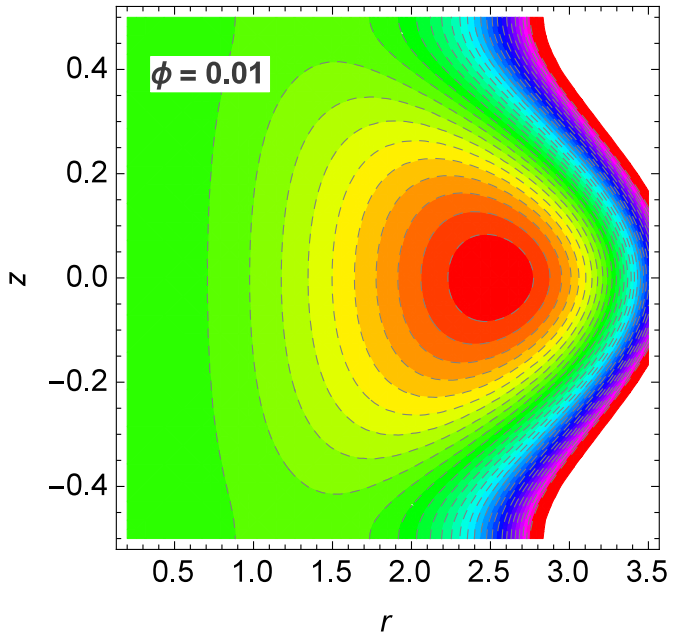

Fig. 11: Stream lines

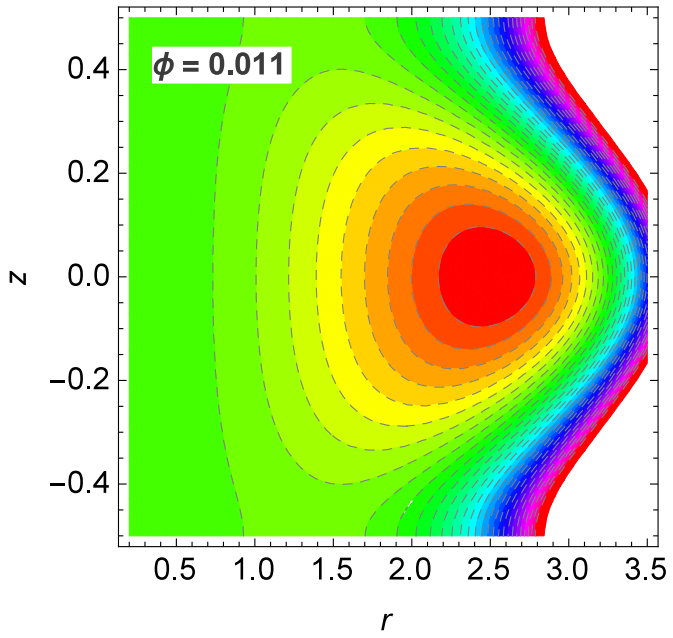

Fig. 12: Stream lines

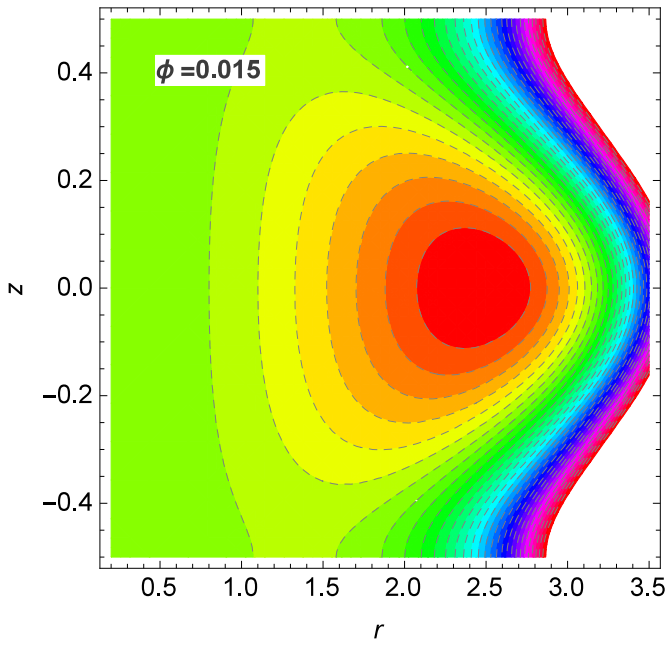

Fig. 13: Stream lines

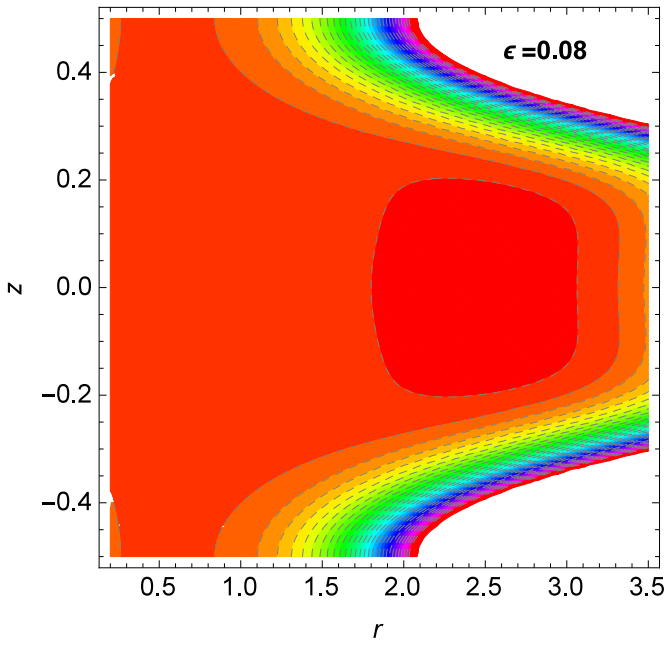

Fig. 14: Stream lines

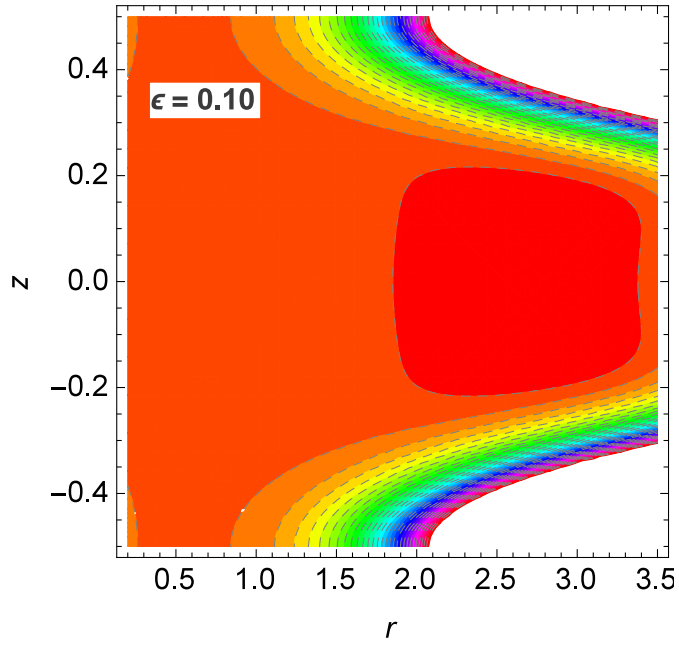

Fig. 15: Stream lines

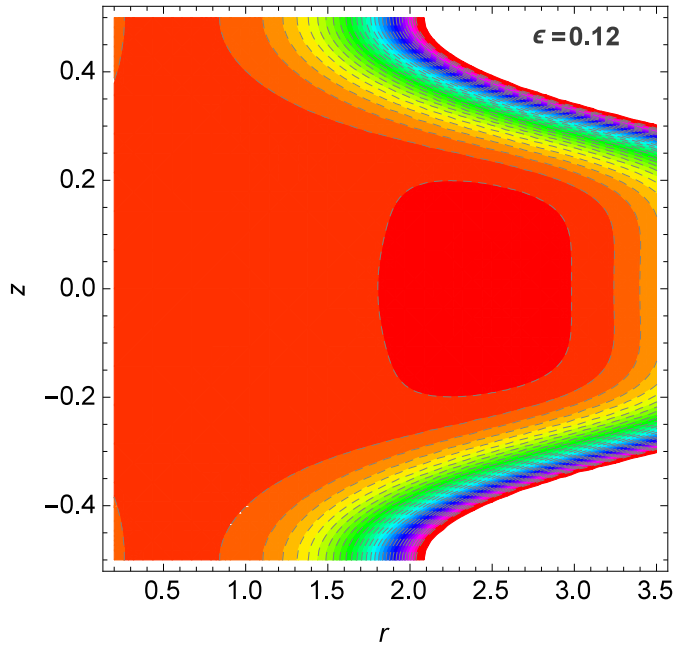

Fig. 16: Stream lines

Chapter 4

Analysis of nanofluid due to trapping along a porous annulus with cilia in the presence of thermal radiation

4.1 Introduction

This chapter is extended work of previous chapter with adding porous annulus and existence of thermal radiation. Mathematical model considered as movement of cilia in presence of endoscopic tube. First we convert system of non linear PDEs into dimensionless non linear ODEs by using non dimensional parameter. Numerical solution is calculated for temperature profile as well as velocity profile. Results for temperature profile, velocity profile, pressure gradient, pressure rise are constructed and evaluated graphically.

4.2 Formulation of model

Consider movement of cilia for two 2-D flow of an incompressible viscous nanofluid in porous annular region with existence of thermal radiation. Continuity and momentum equations can be formulated as

$$\hat{U}_{\hat{R}} + \frac{\hat{U}}{\hat{R}} + \hat{W}_{\hat{Z}} \ = 0 \tag{4.1}$$

$$\rho_{nf} \ \left(\hat{U}_{\hat{t}} + \hat{U}\hat{U}_{\hat{R}} + \hat{W}\hat{U}_{\hat{Z}}\right) = - \hat{P}_{\hat{R}} + \ \mu_{nf} \left(\frac{1}{\hat{R}}\hat{U}_{\hat{R}} + \hat{U}_{\hat{R}\hat{R}} - \ \frac{\hat{U}}{\hat{R}^2} + \hat{U}_{\hat{Z}\hat{Z}}\right) \tag{4.2}$$

$$\rho_{nf}\ (\hat{W}_{\hat{t}} + \hat{U}\hat{W}_{\hat{R}} + \ \hat{W}\hat{W}_{\hat{Z}}) = \ -\hat{P}_{\hat{Z}} + \ \mu_{nf}\ (\frac{1}{\hat{R}}\hat{W}_{\hat{R}} + \hat{W}_{\hat{R}\hat{R}} + \hat{W}_{\hat{Z}\hat{Z}}) - \frac{\mu_{nf}}{k_0}\hat{W} + (\rho\beta)_{nf}\ \hat{g}\ (\hat{T} - T_1)$$

(4.3)

$$\left(\rho\, c_p\right)_{nf}\left(\hat{T}_{\hat{t}} + \ \hat{U}\hat{T}_{\hat{R}} + \ \hat{W}\hat{T}_{\hat{Z}}\right) = k_{nf}\left(\frac{1}{\hat{R}}\hat{T}_{\hat{R}} + \hat{T}_{\hat{R}\hat{R}} + \hat{T}_{\hat{Z}\hat{Z}}\right) + \frac{\mu_{nf}}{k_0}\hat{W}^2 - \frac{\partial q_r}{\partial \hat{R}} + Q_0$$

(4.4)

The radiative heat flux is

$$q_r = \frac{16\sigma^* {T_0}^3}{3k^*}\frac{\partial T}{\partial \tilde{R}}$$

Heat capacity and thermal conductivity of nanofluid express as follow [18, 19]

$$\alpha_{nf}(\rho c_p)_{nf} = k_{nf}, \qquad \mu_{nf}(1-\phi)^{2.5} = \mu_f, \qquad \frac{\rho_{nf}}{\rho_s} = (1-\phi)\frac{\rho_f}{\rho_s}\ +\ \phi$$

$$\frac{(\rho\beta)_{nf}}{\rho_s\beta_s} = (1-\phi)\frac{\rho_f\rho_f}{\rho_s\rho s}\ +\ \phi, \qquad \frac{(\rho c_p)_{nf}}{(\rho c_p)_s} = \phi\ +\ (1-\phi)\ \frac{(\rho\ c_p)_f}{(\rho\ c_p)_s}$$

$$k_{nf}((k_s + 2k_f) + \phi(k_f - k_s)) = k_f((k_s + 2k_f) - 2\phi(k_f - k_s))$$

(4.5)

Table 2: Thermo physical properties of nanoparticles and fluid

Physical properties	Copper	Pure blood
$c_p(\frac{J}{kgK})$	385	3594
$\rho(\frac{kg}{m^3})$	8933	1063
$k(\frac{W}{mk})$	400	0.492
$\beta.10^{-5}(\frac{1}{K})$	1.67	0.18

The internal surface of the tube is ciliated with metachronal waves and the flow happens because of aggregate beating of the cilia. The envelops of the cilia tips can be expressed in mathematical farm:

$$\hat{R} = \hat{g}(\hat{Z},\, \hat{t}) = [a_2 + a_2\epsilon cos(\frac{2\pi}{\lambda}Z^*)] = \hat{R}_2 \tag{4.6}$$

In the light of various examples of cilia movement analysed by Sleigh [20], vertical positions of the cilia tips can be composed as

$$\hat{Z} = \hat{h}(\hat{Z}, \hat{Z}_0, \hat{t}) = \hat{Z}_0 + a_2\alpha\epsilon sin(\frac{2\,\pi}{\lambda}Z^*) \tag{4.7}$$

The vertical and horizontal velocities of cilia are

$$\hat{W} = \frac{\partial \hat{Z}}{\partial \hat{t}} = \frac{\partial \hat{h}}{\partial \hat{t}} + \frac{\partial \hat{h}}{\partial \hat{Z}}\,\frac{\partial \hat{Z}}{\partial \hat{t}} = \frac{\partial \hat{h}}{\partial \hat{t}} + \frac{\partial \hat{h}}{\partial \hat{Z}}\hat{W} \tag{4.8 a}$$

$$\hat{U} = \frac{\partial \hat{R}}{\partial \hat{t}} = \frac{\partial \hat{g}}{\partial \hat{t}} + \frac{\partial \hat{g}}{\partial \hat{Z}}\,\frac{\partial \hat{Z}}{\partial \hat{t}} = \frac{\partial \hat{g}}{\partial \hat{t}} + \frac{\partial \hat{f}}{\partial \hat{Z}}\hat{W} \tag{4.8 b}$$

Solving Eqs (4.6−4.8) we get

$$\hat{W} = \hat{\chi}(\hat{Z},\, \hat{t}) = \frac{\frac{-2\pi}{\lambda}a_2 c\epsilon\alpha\ cos(\frac{2\pi}{\lambda}Z^*)}{1-\frac{2\pi}{\lambda}a_2\epsilon\alpha\ cos(\frac{2\pi}{\lambda}Z^*)} \tag{4.9 a}$$

$$\hat{U} = \frac{\frac{2\pi}{\lambda}a_2 c\epsilon\ sin(\frac{2\pi}{\lambda}Z^*)}{1-\frac{2\pi}{\lambda}a_2\epsilon\alpha\ cos(\frac{2\pi}{\lambda}Z^*)} \qquad \text{at} \quad \hat{R} = \hat{R}_2 \tag{4.9 b}$$

Following transformations are used

$$\hat{r} = \hat{R} \quad , \quad \hat{z} = Z^* \quad , \quad \hat{u} = \hat{U} \quad , \quad \hat{w} = \hat{W} - c \tag{4.10}$$

where $Z^* = \hat{Z} - c\hat{t}$.

Suitable boundary conditions are formulated as

$$\begin{aligned} \hat{W} &= 0 \quad \text{at} \quad \hat{R} = \hat{R}_1 \\ \hat{W} &= \hat{\chi}(\hat{Z}, \hat{t}) \quad \text{at} \quad \hat{R} = \hat{R}_2 = a_2 + a_2\epsilon\cos(\tfrac{2\pi}{\lambda}Z^*) \end{aligned} \tag{4.11}$$

Non dimensional variables are defined as:

$$R = \frac{\hat{R}}{a_2}, \quad p = \frac{a_2^2\hat{p}}{c\lambda\mu_f}, \quad r = \frac{\hat{r}}{a_2}, \quad \delta = \frac{a_2}{\lambda}, \quad Z = \frac{\hat{Z}}{\lambda}, \quad t = \frac{c\hat{t}}{\lambda}, \quad Re = \frac{ac\rho_f}{\mu_f}$$

$$u = \frac{\lambda\hat{u}}{a_2 c}, \quad W = \frac{\hat{W}}{c}, \quad w = \frac{\hat{w}}{c}, \quad r_1 = \frac{\hat{r}_1}{a_2} = \frac{a_1}{a_2} = \xi, \quad \theta = \frac{\hat{T} - \hat{T}_1}{\hat{T}_0 - \hat{T}_1} \quad , \quad U = \frac{\lambda\hat{U}}{a_2 c}$$

$$B = \frac{Q_0 a^2}{k_f(\hat{T}_0 - \hat{T}_1)} \quad , \quad G_r = \frac{g\ \beta_f\ \rho_f\ a^2(\hat{T}_0 - \hat{T}_1)}{c\mu_f}, \qquad r_2 = \frac{\hat{r}_2}{a_2} = 1 + \epsilon\ cos(2\pi z) \tag{4.12}$$

After using dimensionless parameter, applying the condition of low Reynolds number, long wave length approximation and transformation defined in Eqs. (4.10) and (4.12),
Eqs. (4.2−4.4) becomes

$$p_r \quad = \quad 0 \tag{4.13}$$

$$-p_z + \frac{\mu_{nf}}{\mu_f}\left(w_{rr} + \frac{1}{r}w_r - (w+1)\sigma^2\right) + \frac{(\rho\beta)_{nf}}{(\rho\beta)_f}G_r\theta = 0 \tag{4.14}$$

$$\frac{\alpha_{nf}}{\alpha_f}(\frac{1}{r}\theta_r + (1+Rn)\theta_{rr} + \sigma^2 E_m(w{+}1)^2) + B\frac{(\rho c_p)_f}{(\rho c_p)_{nf}} = 0 \tag{4.15}$$

where

$$\sigma^2 = \frac{{a_2}^2}{k_0}, \quad E_m = \frac{c^2\mu_{nf}}{k_{nf}(\tilde{T_0} - \tilde{T_1})}, \quad Rn = \frac{16\sigma^* {T_0}^3}{3k^*}\frac{\sigma_f}{k_{nf}}, \quad \sigma_f = \frac{a_2^2}{(\tilde{T_0} - \tilde{T_1})}$$

Boundary conditions after dimensionless parameters are

$$w = -1{-}2\pi\epsilon\alpha\delta cos(2\pi z) \text{ at } r = r_2 \tag{4.16}$$

$$w = -1 \text{ at } r = r_1 \tag{4.17}$$

$$\theta = 1 \text{ at } r = r_1 \ , \theta = 0 \text{ at } \quad r = r_2 \tag{4.18}$$

$$u = 2\pi\epsilon \sin(2\pi z){+}(2\pi)^2\epsilon\alpha\delta \cos(2\pi z) sin(2\pi z) \text{ at } r = r_2 \tag{4.19}$$

Table 3: Velocity profile for $r_1 = 0.1$, $\sigma = 0.1$, $Em = 0.1$, $z = 0.08$, $\Phi = 0.02$, $\epsilon = 0.05$,$Rn = 1$, $B = 0.17$, $\delta = 0.11$, $\alpha = 0.02$

r	$G_r = 1$ w(r)	$G_r = 2$ w(r)	$G_r = 3$ w(r)	$G_r = 4$ w(r)
0.1	-1	-1	-1	-1
0.2	-0.958843	-0.917463	-0.876083	-0.834703
0.3	-0.946129	-0.891910	-0.837691	-0.783472
0.4	-0.946314	-0.892196	-0.838078	-0.783960
0.5	-0.953436	-0.906381	-0.859325	-0.812270
0.6	-0.964075	-0.927616	-0.891157	-0.854697
0.7	-0.975826	-0.951087	-0.926347	-0.901608
0.8	-0.986787	-0.972988	-0.959189	-0.945391
0.9	-0.995347	-0.990096	-0.984844	-0.979592
1	-1.000080	-0.999550	-0.999022	-0.998494

Table 4: Velocity profile for $r_1 = 0.1$, $\sigma = 0.1$, $G_r = 3$, $Em = 0.1$, $z = 0.08$, $\epsilon = 0.05$, $Rn = 1$, $B = 0.17$, $\delta = 0.11$, $\alpha = 0.02$

r	$\phi = 0.01$ w(r)	$\phi = 0.02$ w(r)	$\phi = 0.03$ w(r)	$\phi = 0.04$ w(r)
0.1	-1	-1	-1	-1
0.2	-0.911467	-0.876083	-0.842582	-0.81092
0.3	-0.884048	-0.837691	-0.793808	-0.752338
0.4	-0.884341	-0.838078	-0.794249	-0.752913
0.5	-0.899544	-0..859325	-0.821262	-0.785300
0.6	-0.922314	-0.891157	-0.861673	-0.833822
0.7	-0.947485	-0.926347	-0.906348	-0.887458
0.8	-0.970978	-0.959189	-0.948038	-0.937506
0.9	-0.989330	-0.984844	-0.980601	-0.976595
1	-0.999473	-0.999022	-0.998596	-0.998193

Table 5: Temperature profile for $r_1 = 0.1$, $\sigma = 0.1$, $G_r = 1$, $Em = 0.5$, $z = 0.03$, $\epsilon = 0.05$, $Rn = 1$, $B = 6$, $\delta = 0.11$ $\alpha = 0.02$

r	$\phi = 0.02$ $\theta(r)$	$\phi = 0.04$ $\theta(r)$	$\phi = 0.06$ $\theta(r)$	$\phi = 0.08$ $\theta(r)$
0.1	1	1	1	1
0.2	0.976894	0.967749	0.959255	0.951346
0.3	0.933736	0.919010	0.905333	0.892596
0.4	0.871104	0.853156	0.836486	0.820962
0.5	0.789224	0.769945	0.752040	0.735365
0.6	0.688211	0.669254	0.651647	0.635250
0.7	0.568133	0.551008	0.535101	0.520289
0.8	0.429036	0.415159	0.402270	0.390267
0.9	0.270950	0.261674	0.253059	0.245036
1	0.093897	0.090529	0.087400	0.084487

4.3 Graphical results

4.3.1 Velocity profile

This section consist of plots showing the influence of various physical parameters appearing the considered flow problem. Grashof number G_r, porosity parameter σ^2, nanoparticle volume fraction ϕ, thermal radiation Rn, and r_1 have been varied for analysis of velocity in Figs. (17 - 21). The numerical tables (see Tables 3 and 4) are also presented to describe the behaviour of velocity against the above said parameters.

It is depicted from Fig. (17) that velocity profile extended with increase in nanoparticle volume fraction. The reason behind the state is that nanoparticle has extended the thermal conductivity. Fig. (18) identifies influence of Grashof number on velocity profile. It is apparent that with rise in Grashof number causes boost in velocity profile. Because buoyancy forces play an important role to create the disturbance in the given fluid for given domain. Fig. (19) exhibits the impact of porosity parameter on velocity profile. Since the flow in porous medium resist so velocity profile decline, so velocity profile decline with higher values of σ. Fig. (20) identifies the effects of thermal radiation on velocity profile. It is observed that velocity profile increase with rising values of Rn. Radiation parameter increased the momentum of fluid molecule which caused the increase in velocity. Fig. (21) demonstrates the change of velocity with higher values of r_1. It is noticed that with increasing values of r_1 velocity profile reduce.

4.3.2 Temperature profile

Plot in Figs. (22 - 24) are prepared to see changes in profile of temperature for influential parameters namely heat source B, nanoparticle volume frac-

tion ϕ, radiation parameter Rn. It can be depicted from Fig. (22) that with increasing values of B temperature profile extended. The effects of nanoparticle volume fraction on temperature profile are shown in Fig. (23). By adding the high concentration of nanoparticle velocity of fluid molecules will show the low momentum due to dense space. Fig. (24) exposes the behaviour of velocity by rising values of thermal radiation parameter. It is discovered from Fig. (24) that temperature profile declines with increase in values of Rn. Radiation plays an inverse role in temperature profile compared to velocity profile.

4.3.3 Pressure gradient

Pressure gradient describes the rate of flow in the direction of pressure changes. Pressure gradient is plotted in Figs. (25 - 27) for distinguish values of nanoparticle volume fraction, cilia length and porosity parameter. In Fig. (25) it is observed that pressure gradient is reduced with increasing values of σ. Fig. (26) represent that by rising values of ϕ pressure gradient declines. Fig. (27) illustrates that pressure gradient is extended with increase in cilia length.

4.3.4 Pressure rise

Figs. (28 - 30) illustrate the behaviour of pressure rise versus various values of nanoparticle volume fraction, cilia length and porosity parameter. Figs. (28 - 29) indicate that by taking higher values of σ and ϕ pressure rise is found to be increase in domain Q $\in [-1,\ 0]$ and on the other hand it decreases in the domain Q $\in [0,\ 1]$. From these figures on can judge that increase in the flow rate causes increase in pressure rise per wave length in the narrow pumping area due to less volume the heat transfer increases

and pressure rise enhances. And inverse behaviour is observed in the wider pumping domain. It is perceive from Fig. (30) that by increasing cilia length parameter pressure rise is rises in region Q $\in [0,\ 1]$in region Q $\in [-1,\ 0.1]$ and decline in Q $\in [0.1,\ 1]$.

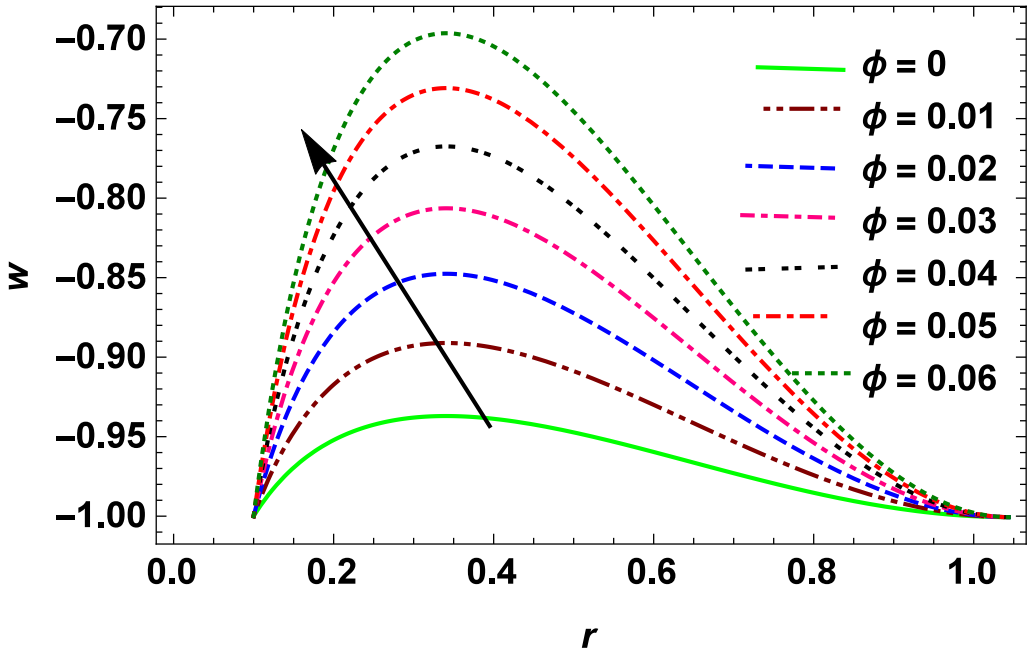

Fig. 17: Velocity profile for variation of ϕ

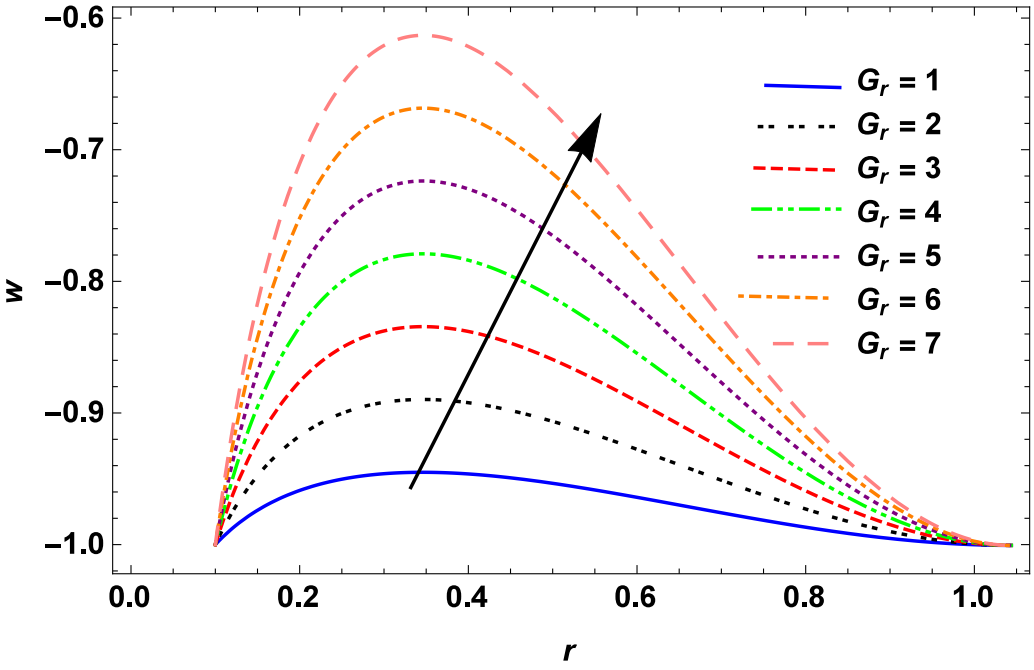

Fig. 18: Velocity profile for variation of G_r

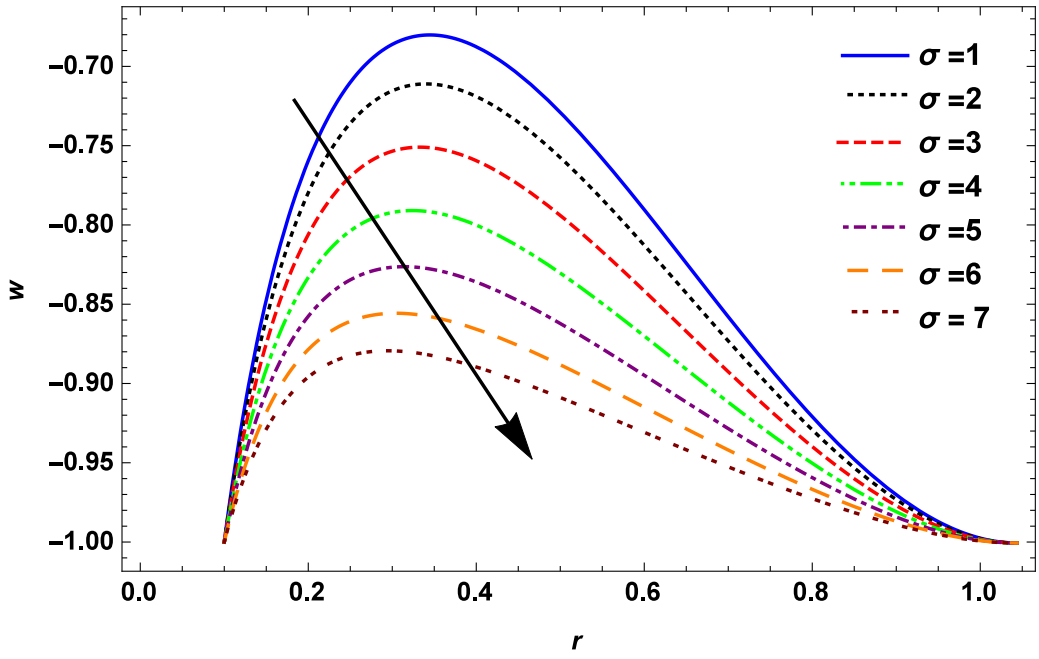

Fig. 19: Velocity profile for variation of σ

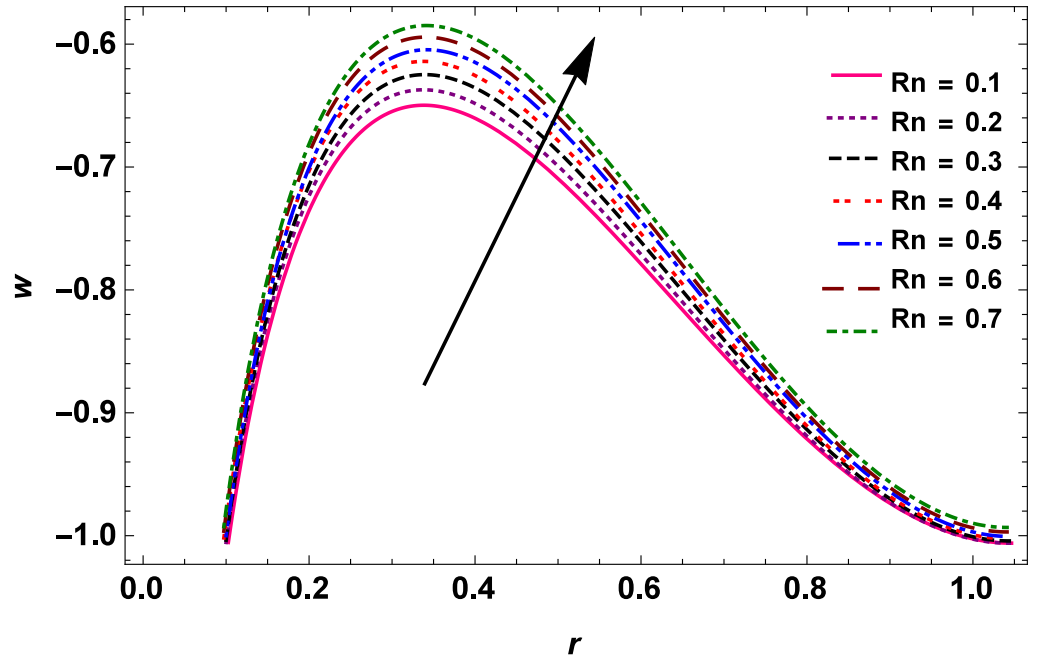

Fig. 20: Velocity profile for variation of Rn

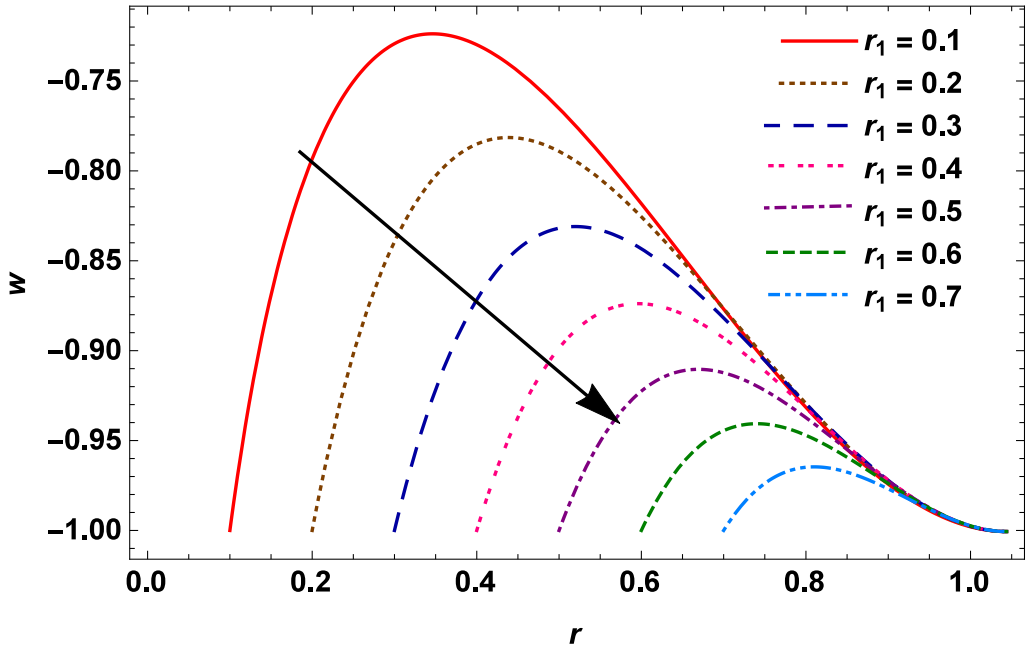

Fig. 21: Velocity profile for variation of r_1

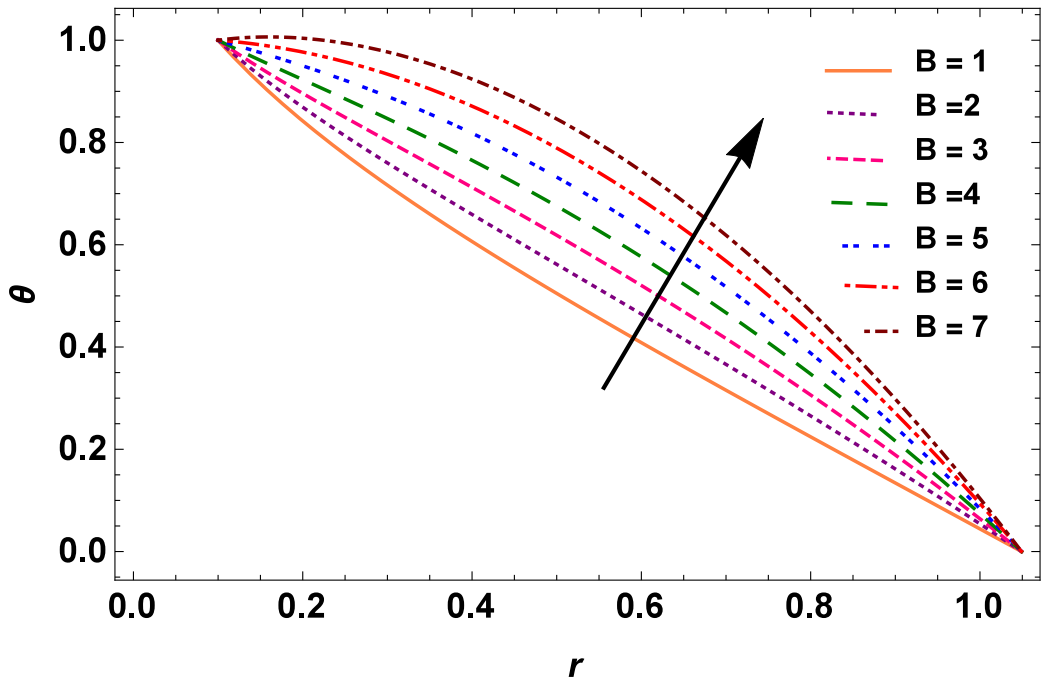

Fig. 22: Temperature profile for variation of B

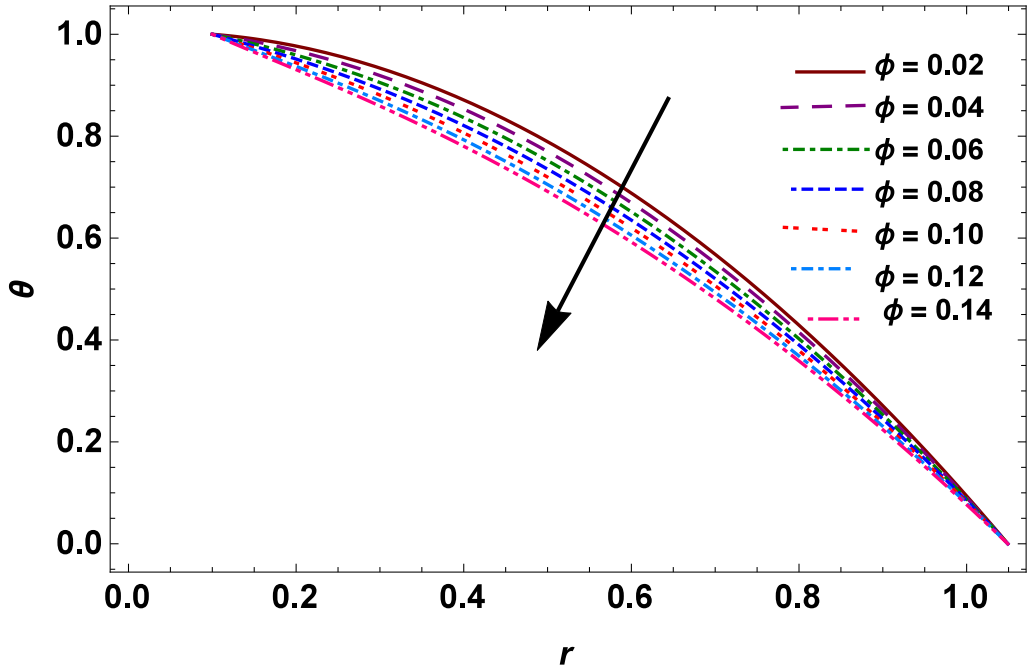

Fig. 23: Temperature profile for variation of ϕ

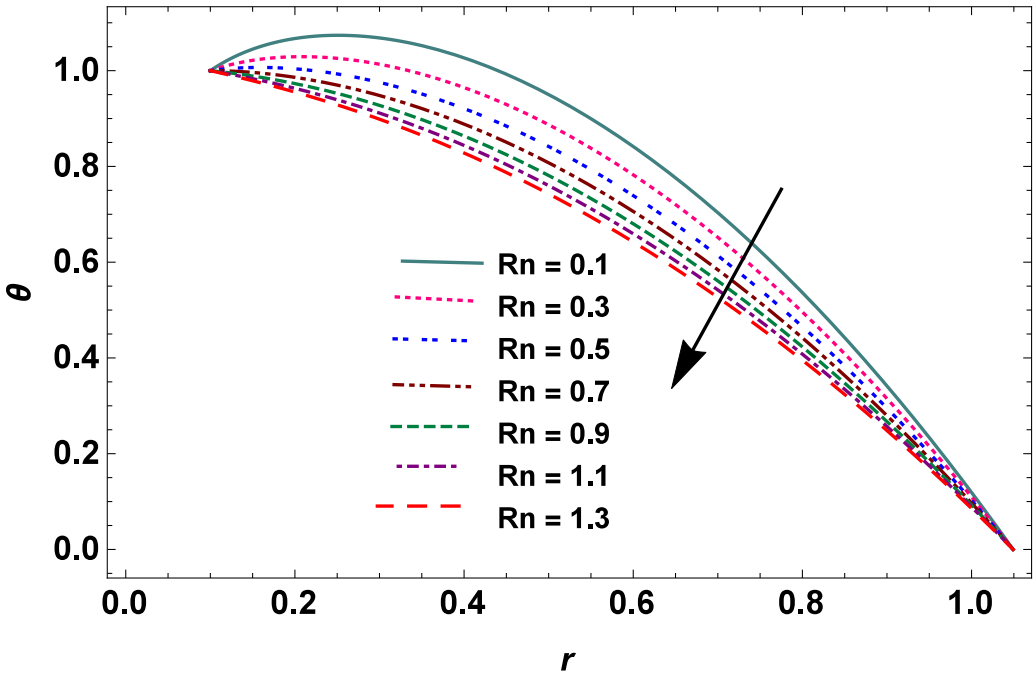

Fig. 24: Temperature profile for variation of Rn

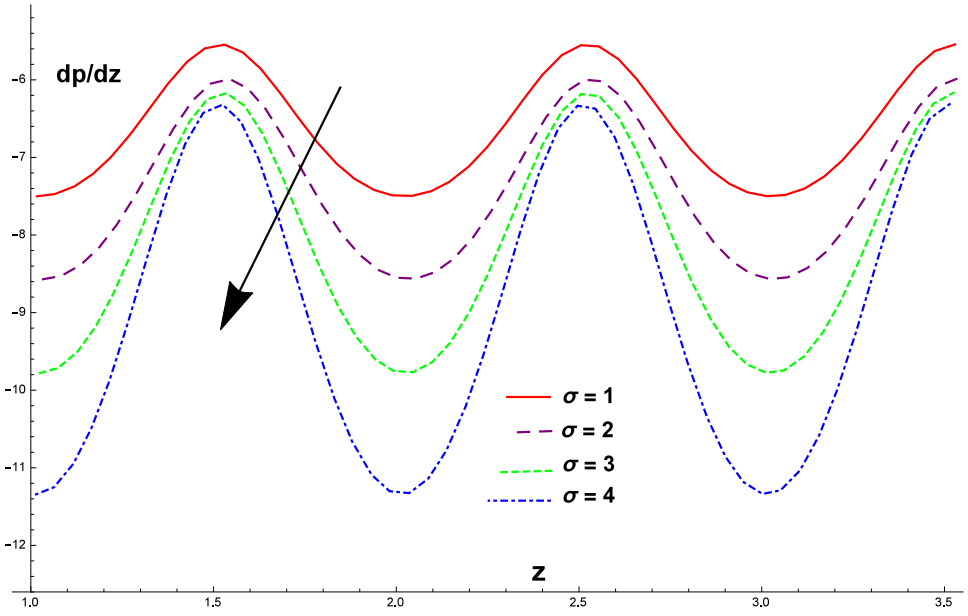

Fig. 25: Pressure gradient for variation of σ with $\phi = 0.02$

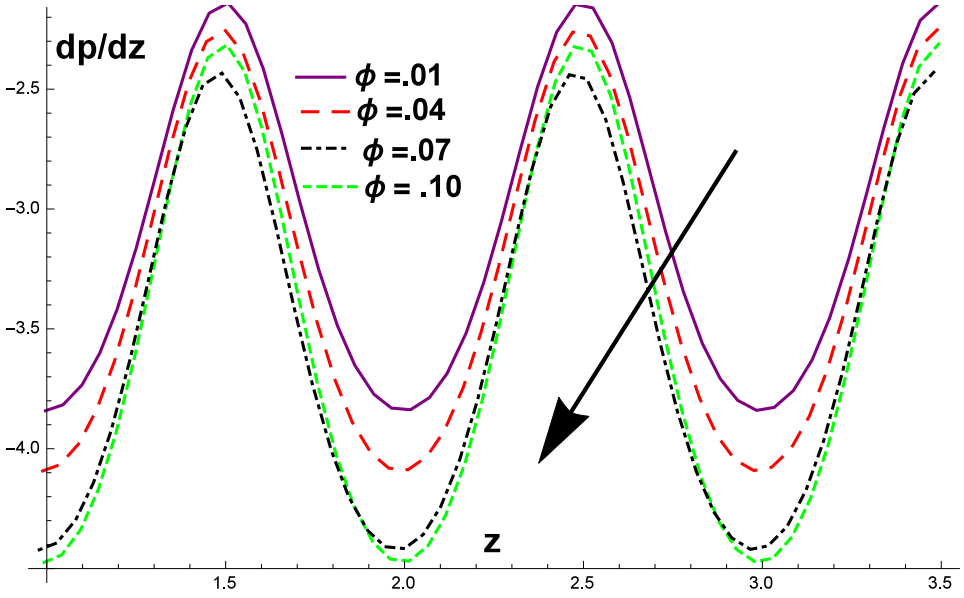

Fig. 26: Pressure gradient for variation of ϕ with $\sigma = 0.01$

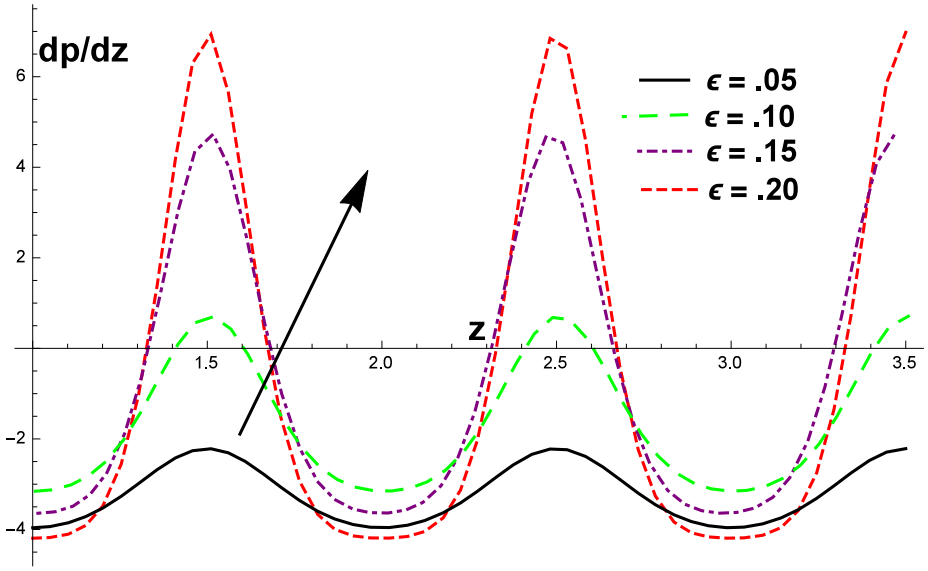

Fig. 27: Pressure gradient for variation of ϵ with $\phi = 0.02$, $\sigma = 0.01$

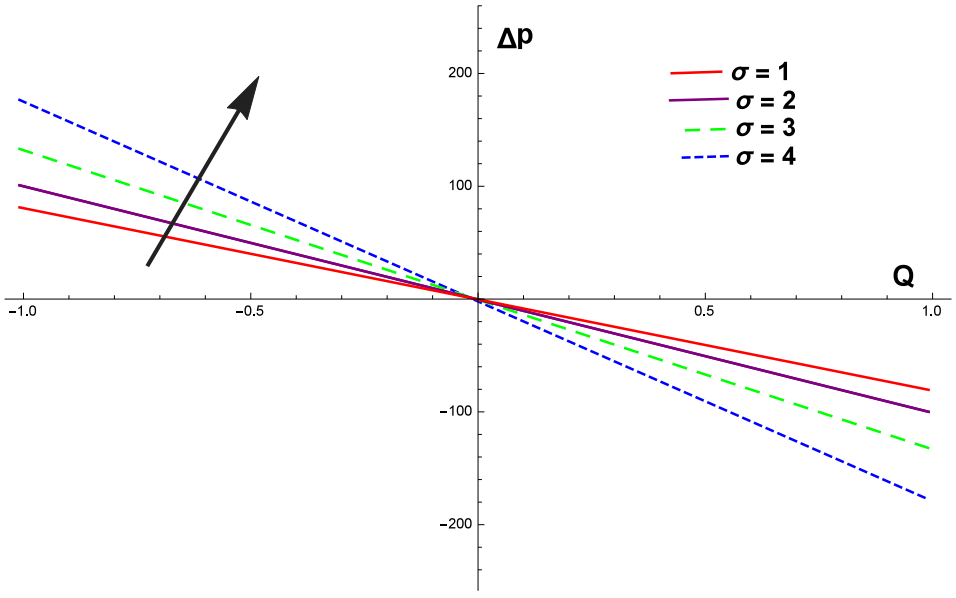

Fig. 28: Pressure rise for variation of σ with $\phi = 0.02$

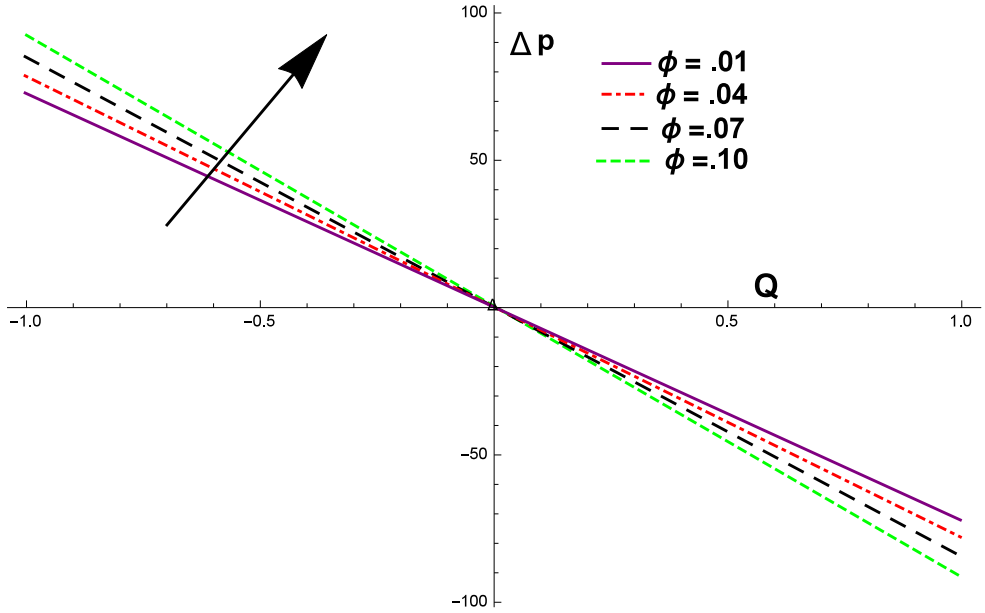

Fig. 29: Pressure rise for variation of ϕ with $\sigma = 0.01$

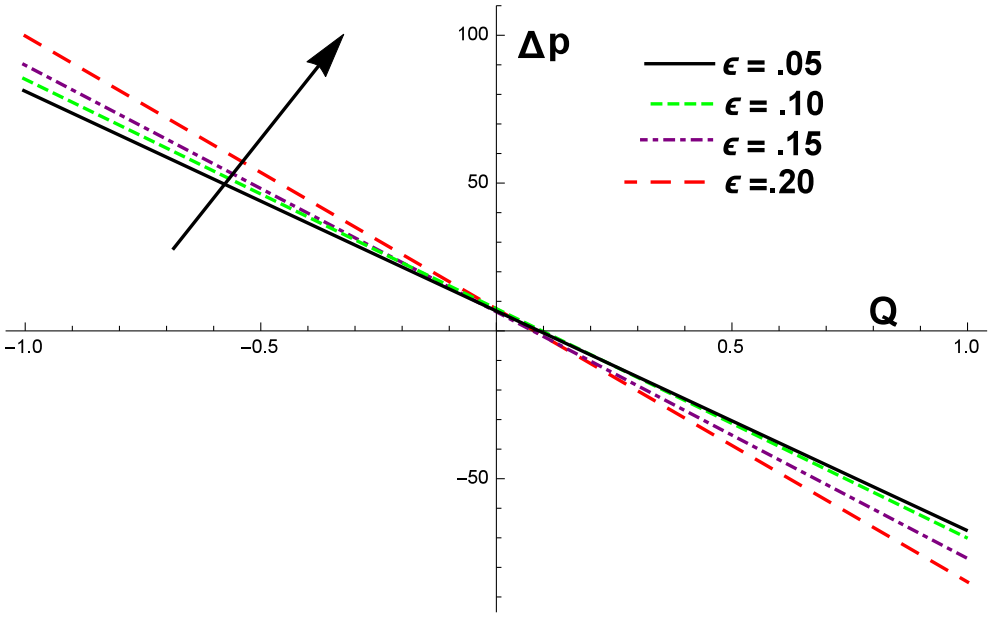

Fig. 30: Pressure rise for variation of ϵ with σ with $\phi = 0.02$

Chapter 5

Conclusion

In Present study we consider results of viscous nanofluid due to cilia motion in porous annulus with presence of thermal radiation. Major findings are

- Velocity profile increases with rising values of Grashof number, Volume fraction of nanoparticle, radiation factor.
- Velocity profile decline with rising values of porosity parameter.
- Temperature of fluid is decline when nanoparticle is added to base fluid and thermal radiation is added.
- Temperature of fluid is extended with increasing the values of heat source parameter.
- Pressure gradient reduces for rising values of both ϕ and σ.
- Pressure gradient is rises when we extend length of cilia.
- Pressure rise increases for various values of ϕ, ϵ, and σ.

References

[1] Latham, T. W. (1966). Fluid motion in peristaltic pumps, M S (Doctoral dissertation, Thesis, MIT, Cambridge, MA).

[2] Shapiro, A. H. (1967). Pumping and retrograde diffusion in peristaltic waves. In Proceedings of the workshop in ureteral reflux in children, Washington, DC (pp. 109-126).

[3] Barton, C., & Raynor, S. (1968). Peristaltic flow in tubes. The Bulletin of mathematical biophysics, 30(4), 663-680.

[4] Shapiro, A. H., Jaffrin, M. Y., & Weinberg, S. L. (1969). Peristaltic pumping with long wavelengths at low Reynolds number. Journal of fluid mechanics, 37(4), 799-825.

[5] Yin, F., & Fung, Y. C. (1969). Peristaltic waves in circular cylindrical tubes. Journal of Applied Mechanics, 36(3), 579-587.

[6] Jaffrin, M. Y. (1973). Inertia and streamline curvature effects on peristaltic pumping. International Journal of Engineering Science, 11(6), 681-699.

[7] Jaffrin, M. Y., & Shapiro, A. H. (1971). Peristaltic pumping. Annual

review of fluid mechanics, 3(1), 13-37.

[8] Takabatake, S., Ayukawa, K., & Mori, A. (1988). Peristaltic pumping in circular cylindrical tubes: a numerical study of fluid transport and its efficiency. Journal of Fluid Mechanics, 193, 267-283.

[9] Mekheimer, K. S. (2008). Peristaltic flow of a couple stress fluid in an annulus: application of an endoscope. Physica A: Statistical Mechanics and its Applications, 387(11), 2403-2415.

[10] Agrawal, H. L., & Anawaruddin. (1984). Cilia transport of bio-fluid with variable viscosity. INDIAN JOURNAL OF PURE & APPLIED MATHEMATICS, 15(10), 1128-1139.

[11] Barton, C., & Raynor, S. (1967). Analytical investigation of cilia induced mucous flow. The Bulletin of mathematical biophysics, 29(3), 419-428.

[12] Jahn, T. L., & Bovee, E. C. (1965). Movement and locomotion of microorganisms. Annual Reviews in Microbiology, 19(1), 21-58.

[13] Jahn, T. L., & Bovee, E. C. (1967). Motile Behaviour of Protozoa, In reesearch in proto-zoology, Vol. 1.

[14] Vélez-Cordero, J. R., & Lauga, E. (2013). Waving transport and propulsion in a generalized Newtonian fluid. Journal of Non-Newtonian Fluid Mechanics, 199, 37-50.

[15] Rydholm, S., Zwartz, G., Kowalewski, J. M., Kamali-Zare, P., Frisk, T., & Brismar, H. (2010). Mechanical properties of primary cilia regulate the response to fluid flow. American Journal of Physiology-Renal Physiology, 298(5), F1096-F1102.

[16] Basten, S. G., & Giles, R. H. (2013). Functional aspects of primary cilia in signaling, cell cycle and tumorigenesis. Cilia, 2(1), 6.

[17] Nadeem, S., & Sadaf, H. (2015). Trapping study of nanofluids in an annulus with cilia. AIP Advances, 5(12), 127204.

[18] Akbar, N. S., & Butt, A. W. (2014). CNT suspended nanofluid analysis in a flexible tube with ciliated walls. The European Physical Journal Plus, 129(8), 174.

[19] Yasin, M., Hafizi, M., Nazar, R., Ismail, F., & Pop, I. (2013). Mixed Convection Boundary Layer Flow Embedded in a Thermally Stratified Porous Medium Saturated by a Nanofluid. Advances in Mechanical Engineering (Hindawi Publishing Corporation).

[20] Sanderson, M. J., & Sleigh, M. A. (1981). Ciliary activity of cultured rabbit tracheal epithelium: beat pattern and metachrony. Journal of Cell Science, 47(1), 331-347.

Analysis of nanofluid flow due to trapping along a porous annulus with cilia in the presence of thermal radiation

ORIGINALITY REPORT

18%	6%	13%	13%
SIMILARITY INDEX	INTERNET SOURCES	PUBLICATIONS	STUDENT PAPERS

PRIMARY SOURCES

1	Submitted to Higher Education Commission Pakistan Student Paper	3%
2	S. Nadeem, Hina Sadaf. "Trapping study of nanofluids in an annulus with cilia", AIP Advances, 2015 Publication	2%
3	Nadeem, S., and Hina Sadaf. "Theoretical Analysis of Cu-Blood Nanofluid for Metachronal Wave of Cilia Motion in a Curved Channel", IEEE Transactions on NanoBioscience, 2015. Publication	1%
4	article.sciencepublishinggroup.com Internet Source	1%
5	Akbar, Noreen Sher, and Adil Wahid Butt. "Entropy generation analysis for metachronal beating of ciliated Cu-water nanofluid with magnetic field", International Journal of	1%